

# Influence of initial soil moisture in a Regional Climate Model study over West Africa. Part 2: Impact on the climate extremes.

Brahima KONÉ<sup>1</sup>, Arona DIEDHIOU<sup>1, 2</sup>, Adama Diawara<sup>1</sup>, Sandrine Anquetin<sup>2</sup>, N'datchoh Evelyne Touré<sup>1</sup>, Adama Bamba<sup>1</sup> and Arsene Toka Koba<sup>1</sup>

<sup>1</sup>LAPAMF, Université Félix Houphouët Boigny, Abidjan, Côte d'Ivoire

<sup>2</sup>Univ. Grenoble Alpes, IRD, CNRS, Grenoble INP, IGE, F-38000 Grenoble, France

*Correspondence to:* Arona DIEDHIOU (arona.diedhiou@ird.fr)

## **Abstract.**

The influence of the initial soil moisture conditions on the climate extreme over West Africa is investigated using the fourth generation of Regional Climate Model version 4 (non-hydrostatic) coupled to the version 4.5 of the Community Land Model (RegCM4-CLM4.5) at 25 km spatial resolution. Sensitivity studies was carried out during 5 years from 2001 to 2005, with initial soil moisture conditions prescribed on June 1st and simulations performed over 4 months (120 days) from June to September (JJAS). Results have been presented for two extreme years 2003 (above normal precipitation year) and 2004 (below normal precipitation year) in the aim to estimate the limits of the impact of internal soil moisture forcing on the new non-hydrostatic dynamical core of RegCM4. We initialized the control runs with the reanalysis soil moisture of the European Centre Meteorological Weather Forecast's reanalysis of the 20th century (ERA20C), while for the dry and wet experiments, we initialized the soil moisture respectively at the wilting points and field capacity. The impact on extreme precipitation indices of the initial soil moisture, especially over the central Sahel, is linear, i.e. dry (wet) experiments tend to decrease (increase) precipitation extreme indices only for precipitation indices related to the number of precipitation events, not for those related to the intensity of precipitation events. The impact on temperature extremes of the initial soil moisture conditions is more significant compared to precipitation extremes. Initial soil moisture conditions unequally affect daily minimum and maximum temperature. A stronger impact is found on maximum temperature than minimum temperature. Over the entire West African domain, wet (dry) experiments cause a decrease (increase) in maximum temperature. The strongest impacts on minimum temperature indices are found mainly in wet experiments,

32 on the Sahara where we found the higher values of the maximum and minimum daily  
33 minimum temperature indices (resp. TN<sub>x</sub> and TN<sub>n</sub>). The performance of RegCM4-CLM4.5  
34 in simulating the ten (10) extreme rainfall and temperature indices used in this study is also  
35 highlighted.

## 36 **1 Introduction**

37 West Africa experienced large rainfall variability during the late 1960s. This variability leads  
38 often to flooding events, severe drought and regional heatwaves. Such extreme hydro-climatic  
39 events have major economic, environmental, and societal impacts (Easterling et al., 2000),  
40 Larsen (2003)). In recent years, climate extremes have attracted much interest because they  
41 are expected to occur more frequently (International Panel on Climate Change (IPCC), 2012)  
42 than changes in mean climate. Yan and Yang (2000) show that for a large number of cases,  
43 the extreme climate changes were 5 to 10 times greater than climate mean change. Many key  
44 factors or physical mechanisms could be possible causes of the increase in climate extremes  
45 (Nicholson (1980); Le Barbé et al., 2002), such as the effect of increasing greenhouse gases in  
46 the atmosphere on the intensification of hot extremes (IPCC, 2007), the sea surface  
47 temperature (SST) anomalies (Fontaine and Janicot 1996; Folland et al., 1986), and land  
48 surface conditions (Philippon et al., 2005; Nicholson (2000)). In addition, smaller-scale  
49 physical processes, including the interactions of the coupling of land-atmosphere, can lead to  
50 changes in climate extremes. For the European summer, the influence of soil moisture in the  
51 coupling of land-atmosphere using regional climate model and focused on the extremes and  
52 trends in precipitation and temperature have been studied by Jaeger and Seneviratne (2011).  
53 For extreme temperatures, their studies have shown that interactions of soil moisture and  
54 climate have a significant impact, while for extreme precipitation, they only influence the  
55 frequency of wet days. Over Asia, Liu et al. (2014) studied the impact on subsequent  
56 precipitation and temperature of soil moisture anomalies using a regional climate model. They  
57 show that wet (dry) experiences decrease (increase) the hot extremes, decrease (increase) the  
58 drought extremes, and increase(decrease) the cold extremes in a zone of strong soil moisture-  
59 atmosphere coupling. However, none of these papers intended to examine the impacts of the  
60 initial soil moisture conditions on subsequent climate extreme using a regional climate model  
61 over West Africa. In part 1, the influence of initial soil moisture on the climate mean was  
62 based on performance assessment of the Regional Climate Model coupled with the complex  
63 Community Land Model (RegCM4-CLM4.5) done by Koné et al. (2018) where the ability of

64 the model to reproduce the climate mean has been validated. However, in part 2, before  
65 starting to study the influence of initial soil moisture on the climate extremes, it was needed to  
66 assess first the performance of RegCM4-CLM4.5 in simulating the ten (10) temperature  
67 indices and extreme rainfall used in this study. This has never been done before over Africa.  
68 That's why we separate in two parts, to ease the reading and to come up with papers of  
69 reasonable length. The paper is organized as follows: section 2 describes the model RegCM4,  
70 the experimental design and methodology used in this study; section 3 presents the  
71 assessment of RegCM4-CLM4.5 in climate extremes simulation and the impacts on climate  
72 extremes of the initial soil moisture conditions; and section 4 documents the conclusions.

## 73 **2. Model, experimental design and methodology**

### 74 **2.1 Model description and numerical experiment**

75 The fourth generation of the Regional Climate Model (RegCM4) of the International Centre  
76 for Theoretical Physics (ICTP) is used in this study. Since this version, the physical  
77 representations have been subject to a continuous process of implementation and  
78 development. The release used in this study is RegCM4.7. The non-hydrostatic dynamical  
79 core of the MM5 (Mesoscale Model version 5, Grell et al., 1994) has been ported to RegCM4  
80 while maintaining the existing hydrostatic core. We selected in this study the non-hydrostatic  
81 as the model dynamical core. RegCM4 is a limited-area model using a vertical grid sigma  
82 hydrostatic pressure coordinate and a horizontal grid of Arakawa B-grid (Giorgi et al., 2012).  
83 The radiation scheme is from the NCAR-CCM3 (National Center for Atmospheric Research  
84 and the Community Climate Model Version 3) (Kiehl et al., 1996) and the aerosols  
85 representation is from Zakey et al. (2006) and Solmon et al. (2006). The large-scale  
86 precipitation scheme used in this study is from Pal et al. (2000), the moisture scheme is called  
87 the SUBgrid EXplicit moisture scheme (SUBEX) which considers the sub-grid variability in  
88 clouds, the accretion and evaporation processes for stable precipitation is from Sundqvist et  
89 al. (1989). The sensible heat and water vapor in the planetary boundary layer over land and  
90 ocean, turbulent transports of momentum are from Holtslag et al. (1990). The heat and  
91 moisture and the momentum of ocean surfaces fluxes are from Zeng et al. (1998). Convective  
92 precipitation and the land surface processes in RegCM4.7 are represented in several options.  
93 Based on Koné et al. (2018), the convective scheme of Emanuel (Emanuel, 1991) is used. The  
94 parameterization of the land surface processes is from CLM4.5 (Oleson et al., 2013). In each  
95 grid cell of CLM4.5, there is 16 different plant functional types and 10 soil layers (Lawrence

96 et al., 2011; Wang et al., 2016). The integration of RegCM4 over the West African domain is  
97 shown in Fig. 1 with 18 vertical levels and 25 km (182x114 grid points; from 20°W-20°E and  
98 5°S-21°N) of horizontal resolution. The European Centre for Medium-Range Weather  
99 Forecasts reanalysis (EIN75; Uppala et al., 2008; Simmons et al., 2007) provides the initial  
100 and boundary conditions. The Sea Surface Temperatures (SSTs) are derived from the  
101 National Oceanic and Atmosphere Administration optimal interpolation weekly (NOAA -  
102 OI\_WK) (Reynolds et al., 1996). The topography is derived from States Geological Survey  
103 (USGS) Global Multi-resolution Terrain Elevation Data (GMTED; Danielson et al., 2011) at  
104 the spatial resolution of 30 arc-second which is an update of the Global Land Cover  
105 Characterization (GTOPO; Loveland et al., 2000) dataset.

106 The sensitivity of the initial soil moisture does not exceed four months (Hong and Pan., 2000;  
107 Kim and Hong, 2006). (Hong and Pan., 2000; Kim and Hong, 2006). As mentioned in Part I,  
108 we performed these sensitivity studies to the initial conditions of soil moisture over our West  
109 African domain for June-July-August-September (JJAS) from 2001 to 2005 with a focus on  
110 two contrasted years 2003 (above normal precipitation year) and 2004 (below normal  
111 precipitation year). The two years 2003 and 2004 (resp. the wettest and the driest years among  
112 the 5 years) have been selected in the aim to estimate the limits of the impact of internal soil  
113 moisture forcing on the new dynamical core non-hydrostatic of RegCM4. Several previous  
114 studies used two extreme years for their sensitivity study of initial soil moisture condition on  
115 the models (e.g Hong et al., 2000; Kim and Hong, 2006). We set up an ensemble of 3  
116 experiments each with simulations starting from June 1st to September 30th. For each  
117 experiment, we applied (i) a reference initial soil moisture condition, (ii) then a wet initial soil  
118 moisture condition, and finally (iii) a dry initial soil moisture condition. Kang et al. (2014) by  
119 comparing different land surface schemes (BATS and CLM3) and different periods of spin-up  
120 to simulate June – July – August precipitations recommended 7 days as spin-up period. In this  
121 study, we used CLM4.5 as land surface scheme (Oleson et al., 2013) which has a more  
122 complex design. The first 7 days (Kang et al., 2014) are excluded in the analysis as a spin-up  
123 period. We used the soil moisture from the reanalysis of the European Centre Meteorological  
124 Weather Forecast's Reanalysis of the 20<sup>th</sup> century (ERA20C) to initialize the control runs.  
125 Wet and dry experiments were initialized for the soil moisture (in volumetric fraction  $m^3.m^{-3}$ )  
126 respectively at the field capacity ( $=0.489$ ) and the wilting point ( $=0.117.10^{-4}$ ) over the West  
127 African derived from ERA20C soil moisture dataset.

## 129 **2.2 Validation datasets and evaluation metrics**

130 Our investigation is focused on the air temperature at 2 m and the precipitation over the West  
131 African domain during the summer of JJAS for 2003 and JJAS 2004. The simulated  
132 precipitation fields are validated with two observation datasets: the Climate Hazards group  
133 Infrared Precipitation Stations (CHIRPS) dataset is from the University of California at Santa  
134 Barbara, available from 1981 to 2020 at the  $0.05^\circ$  high-resolution and the Tropical Rainfall  
135 Measuring Mission 3B43V7 (TRMM) dataset with the  $0.25^\circ$  high-resolution available from  
136 1998 to 2013 (Huffman et al., 2007). We validated the 2 m temperature with two observation  
137 datasets: the global daily temperature from the Global Telecommunication System (hereafter  
138 GTS), gridded at the horizontal resolution of  $0.5^\circ$  for 1979 to 2020 (Fan Y. and Huug van den  
139 Dool, 2008) and daily temperature from ERA-Interim (EIN) reanalysis at  $0.25^\circ$  of horizontal  
140 resolution available from 1979 to 2020 (Dee et al., 2011). For the comparison of the  
141 simulations of the model with observation datasets, we re-gridded all the products to  $0.22^\circ \times$   
142  $0.22^\circ$ . We used an interpolation of the bilinear method for this purpose (Nikulin et al., 2012).  
143 The performance of RegCM4-CLM4.5 to simulate the extreme indices has been carried using  
144 four selected sub-regions (Fig. 1) based on the previous work of Koné et al. (2018), they  
145 correspond to different features of the annual cycle of precipitation. We used the mean bias  
146 (MB), which captures the small-scale differences between the simulation and the observation.  
147 The pattern correlation coefficient (PCC) is also used as a spatial correlation between model  
148 simulations and the observation to indicate the large-scale similarity degree.

149 To quantify the impact of soil moisture anomalies on climate extremes Liu et al. (2014) in  
150 their work over Asia, used the mean biases in 5 subregions, while in our study we used the  
151 mean biases and the probability density function (PDF, Gao et al. (2016); Jaeger and  
152 Seneviratne (2011)) for this purpose to better capture how many grid points are impacted by  
153 initial soil moisture and their highest value.

154 The statistically significant differences has been tested between the control and the sensitivity  
155 experiments, we perform the two-tailed of the student's t-distribution at every grid points as  
156 did by Liu et al. (2014) in a similar work over Asia. Due to the multiplicity problem of  
157 independent tests and the spatial dependency of neighboring grid points, the significant results  
158 can only be seen as a crude estimate. Therefore, we perform the land point's area-weighted

159 fraction with statistical significance of 10% level and we display the seasonally extreme  
160 indices maps during the years 2003 and 2004.

### 161 **2.3. Extreme rainfall and temperature indices**

162 In this study, to investigate the changes in precipitation and temperature in terms of duration,  
163 occurrence and intensity, six extreme temperature and four extreme rainfall indices are  
164 examined using daily data of minimum and maximum temperature and daily rainfall (Table  
165 1). These 10 extreme indices are recommended by the Expert Team on Climate Change  
166 Detection and Indices (ETCCDI, Peterson et al., 2001). We estimated the monthly values of  
167 the indices, which allow investigating of the seasonal variations.

168

## 169 **3. Results and discussion**

### 170 **3.1. Seasonal extreme rainfall**

171 In this section, we analyze six extreme rainfall indices based on daily precipitation in  
172 RegCM4 simulations over West Africa. All precipitation indices are calculated for JJAS 2003  
173 and JJAS 2004. Table 2 summarizes the pattern correlation coefficient (PCC) and the mean  
174 bias (MB) of all precipitation indices studied in this section for TRMM observation and  
175 model simulations derived from control experiments with reanalysis initial soil moisture  
176 ERA20C with respect to CHIRPS observation, calculated for the west Sahel, central Sahel,  
177 Guinea coast and the entire West African domain during the period JJAS 2003 and JJAS  
178 2004.

#### 179 **3.1.1 The index of the number of the wet days (R1mm index)**

180 Figure 2 shows the mean values of the number of the wet days (R1mm index, in days) from  
181 CHIRPS (Fig.2a, d) and TRMM (Fig2b, e) observations and their corresponding simulated  
182 control experiments (Fig2c, f) with the initial soil moisture derived from ERA20C reanalysis.  
183 The two observation datasets CHIRPS (Fig. 2a, d) and TRMM (Fig.2b, e) show a similar  
184 large-scale pattern over the West African domain with a PCC up to 0.98 (Table 2). The  
185 maximum values of the R1mm index are located over the regions of mountains such  
186 Cameroon mountains, Jos plateau and the Guinea highlands, while the minimum values of  
187 R1mm index are found over the Sahel with the number of wet days which decrease gradually  
188 from South to North. However, although the large-scale patterns are similar, at the local scale  
189 some differences are found in term of magnitude and spatial extent of these maxima and  
190 minima. The TRMM datasets underestimate the number of the wet days over the central and



191 west Sahel, and they are overestimated over Guinea coast for both JJAS 2003 and JJAS 2004  
192 (Table 2). For instance, over the central Sahel, we observe a strong mean bias (MB) about -  
193 6.76 and 7.51 days (resp. for JJAS 2003 and JJAS 2004, Table 2), and over the Guinea coast,  
194 the MB reaches 8.89 and 10.44 days (resp. for JJAS 2003 and JJAS 2004, Table 2).

195 The control experiments (Fig.2c, f) reproduce well the large-scale structure of the observed  
196 rainfall with a PCCs values reached 0.96 and 0.95 (resp. for JJAS 2003 and JJAS 2004, Table  
197 2) over the entire West African domain, but do exhibit some biases at the locale scale in term  
198 of spatial extent and magnitude. The control experiment display a large and quite  
199 homogeneous area of maximum values of R1mm index under the latitude 12°N. The control  
200 experiments overestimate the number of wet days over most of the studied domains (Table2).  
201 The largest mean biases are found over the Guinea coast with MB more than 53.16 and 55.46  
202 days (resp. for JJAS 2003 and JJAS 2004, Table 2). This overestimation of the number of wet  
203 days in RegCM4 has been also found by Thanh et al. (2017) with RegCM4 over the Asia  
204 region.

205 Figure 2 (second panel) displays also changes in the R1mm index for JJAS 2003 and JJAS  
206 2004, for dry (Fig.2g and i, resp. for JJAS 2003 and JJAS 2004) and wet experiments (Fig.2h  
207 and j, resp. for JJAS 2003 and JJAS 2004) compared to their control experiments associated,  
208 the dotted area shows changes with statistical significance of 10% level. The dry experiments  
209 (Fig.2g, i) tend to decrease the R1mm index while the wet experiments (Fig.2h, j) tend to  
210 favor an increase of the R1mm index, especially over the central Sahel and a small part of  
211 west Sahel. However, over the Guinea coast sub-region, both wet and dry experiments show a  
212 significant increase of R1mm, although weaker in the dry experiments.

213 For a better quantitative evaluation, Figure 3 shows the PDF distributions of the changes in  
214 R1mm index over the studied domains (Fig.1), during JJAS 2003 and JJAS 2004. The results  
215 essentially confirm the linear impact found over the central Sahel (Fig.3a). The strongest  
216 impact on the R1mm index for the dry (wet) experiments is located over the central (west)  
217 Sahel, with a decrease (an increase) of R1mm index and with a peak at -5 days (10 days) for  
218 JJAS 2003 and JJAS 2004. Over the West Sahel, the Guinea coast and the West African  
219 domain (resp. Fig.3b, c and d), both dry and wet experiments lead to an increase of R1mm  
220 index. For instance, over Guinea coast, a peak is found at 3 days for both wet and dry  
221 experiments. The sensitivity of R1mm index to the contrast of year is shown by the lag  
222 between the peaks of PDFs in wet and dry experiments. The strongest impact of contrast years

223 is found over the west Sahel (Fig.3b) reached 3 days, especially in wet experiments. The wet  
224 year (2003) is more sensitive to R1mm index changes than the dry year (2004).

225 Summarizing the results of this section, RegCM4 overestimates the number of wet days over  
226 most of the domain studied. The strongest linear impact on the R1mm index for the dry (wet)  
227 experiments is found over the central (west) Sahel, with a decrease (an increase) of R1mm  
228 index. The peak is found at -5 days and 10 days, respectively for dry and wet experiments.  
229 This result is in line with previous work which sustained a strong coupling of land and  
230 atmosphere in areas between wet and dry climate regimes (Zhang et al., 2011; Koster et al.,  
231 2006). The impact of the contrast of year is significant on the number of wet days in wet and  
232 dry experiments over west and central Sahel respectively.

233

### 234 3.1.2 The simple daily intensity index (SDII index)

235 We analyzed in this section the SDII index which gives the amount of precipitation mean on  
236 wet days (daily precipitation >1mm). Figure 4 (first panel) is the same as Fig.2 (first panel)  
237 but shows the amount of precipitation mean on wet days (SDII index, in mm.day<sup>-1</sup>). Over the  
238 entire West African domain, the two observations products CHIRPS (Fig.4a, d) and TRMM  
239 (Fig.4b, e) present a similar large-scale pattern with a PCC about 0.86 for both JJAS 2003 and  
240 JJAS 2004 (Table 2). However, the maxima SDII index values are quite different in term of  
241 spatial extension and magnitude. Over the coastline of the Gulf of Guinea, CHIRPS datasets  
242 (Fig.4a, d) depict the highest values of SDII index, more than 25 mm.day<sup>-1</sup> and located. While  
243 the SDII index values, in TRMM datasets not exceed 12 mm.day<sup>-1</sup> over most part of this  
244 region. Over the central and west Sahel, TRMM datasets show large sparse values of SDII  
245 index up to 20 mm.day<sup>-1</sup>, while CHIRPS datasets not exceed 12 mm.day<sup>-1</sup> for both JJAS 2003  
246 and JJAS 2004. The largest biases of TRMM with respect to CHIRPS are found over the  
247 Guinea coast sub-region with MB more than 13 and 14 mm.day<sup>-1</sup> (resp. for JJAS 2003 and  
248 JJAS 2004, Table2). This shows a quite discrepancy among the observation datasets over  
249 West African domain. We have chosen CHIRPS because of its high resolution and mainly  
250 because this product has been widely assessed and used for study of extremes events in West  
251 Africa by Bichet et al. (2018a, b) and Didi et al. (2020).

252 The control experiments (Fig.4 c, f) well reproduce the large-scale pattern of observation  
253 products with a PCC reached 0.73 and 0.77 (resp. in JJAS 2003 and JJAS 2004, Table 2) over  
254 West African domain. However, at the locale scale, some biases are shown. Over most of the  
255 domain studied, the magnitude of SDII index is quite underestimated, not exceed 10 mm.day<sup>-1</sup>



256 <sup>1</sup>, except over the Cameroon mountains (Fig.4c, f). As a result, precipitation events are less  
257 extreme in the control experiments. The largest mean biases are located over the Guinea coast  
258 with MB more than -13.62 and -14.65 mm.day<sup>-1</sup> (resp. for JJAS 2003 and JJAS 2004, Table  
259 2).

260 Figure 4 (second panel) is the same as Fig. 2 (second panel), but displays changes in the  
261 amount of precipitation mean on wet days. Unlike for R1mm index, a change in SDII index is  
262 not linear over all the domains studied. In general, a similar mixture of both increase and  
263 decrease is shown for dry and wet experiments over most of the domains studied (Figure 4,  
264 second panel).

265 Figure 5 displays PDFs of changes in SDII index, as in Fig.3, The PDFs show the peak  
266 centered approximately on zero, this means shows that changes in the amount of precipitation  
267 mean on wet days for wet and dry experiments is not significant. The SDII index is also not  
268 sensitive to the contrast of the year in both wet and dry experiments over the different  
269 domains studied (Fig.5).

270 In summary, the RegCM4 underestimates the amount of precipitation mean on wet days over  
271 all the domain study. It is worth to note that precipitation events simulated by RegCM4 with  
272 the current parameterization are less extreme, the SDII index not exceeding 10 mm.day<sup>-1</sup> over  
273 the entire West African domain. The impact on precipitation amount on wet days of the dry  
274 and wet experiments is not significant and not sensitive to the contrast of year over the entire  
275 domain studied.

276

### 277 **3.1.3 The maximum number of consecutive dry days (CDD index).**

278 The duration of dry spells (CDD index) which represents the maximum number of  
279 consecutive dry days with precipitation less than 1 mm.day<sup>-1</sup> is analyzed in this section.

280 Figure 6 (first panel) is the same as Fig.2 (first panel) but shows the maximum number of  
281 consecutive dry days (CDD index, in day). CHIRPS datasets located the largest values of  
282 CDD index over the Sahara, more than 50 days (Fig.6a, d). While the lowest values are found  
283 over the Guinea coast, with CDD index values less than 8 days. Over the West African  
284 domain, both CHIRPS and TRMM datasets show quite similar large scale features over the  
285 entire West African domain with PCC more than 0.92. However, at the local scale, the  
286 observations datasets exhibit some disparities. In general, these disparities relate only on  
287 spatial extent, especially over the Sahel region. In JJAS 2003, the band of CDD index values  
288 is in the range of [10; 20] days and extended too far into Sahel region for TRMM than

289 CHIRPS. For JJAS 2004, TRMM observation (Fig.6b, e) presents a narrower band of  
290 minimum CDD index values over the Guinea coast around the latitude 10°N than CHIRPS  
291 which extends it over Guinea coast. TRMM observation underestimates the CDD index over  
292 the entire West African domain, with MB about -2.29 and -1.75 days (resp. for JJAS 2003 and  
293 JJAS 2004, table2).

294 The control experiments (Fig.6c, f), over the entire West African domain, well reproduce the  
295 large-scale pattern of the observed rainfall with a PCC more than 0.85 and 0.89 (resp. for  
296 JJAS 2003 and JJAS 2004, Table 1). However, in term of magnitude, some differences are  
297 shown at the locale scale. In general, the control experiments overestimate the CDD index  
298 over the most of the domain studied, except over the Guinea coast (Table2). For instance,  
299 over the West African domain, the control experiments overestimate the CDD index with MB  
300 more than 2.63 and 7 days (resp. for JJAS 2003 and JJAS 2004, table2). The current  
301 parameterization of the model tends to increase the drought extreme over most of the domain  
302 studied, except over Guinea coast where it is too wet.

303 Figure 6 (second panel) is the same as Fig.2 (second panel) but shows changes in the  
304 maximum lengths of consecutive dry spells (CDD index). The initial soil moisture impact on  
305 the consecutive dry spell is linear over the central and west Sahel (Fig 6, second panel), the  
306 dry (wet) experiments tends to increase (decrease) the maximum lengths of consecutive dry  
307 spell (CDD index). However, particularly over Guinea coast, the dry and wet experiments  
308 lead to a decrease.

309 Figure 7 is the same as Fig.3 but displays the PDF distribution of the changes in the CDD  
310 index. The impact on CDD index is linear over the central and west Sahel. For instance, over  
311 the central Sahel, peaks are obtained at -6 and 2 days respectively for dry and wet experiences  
312 (Fig.7a). The weaker and non-linear impact is found over the Guinea coast and the West  
313 African domain. For instance, over the Guinea coast, a decrease in CDD index values is found  
314 with a peak not exceeding 2 days for both wet and dry experiments (Fig.7c). The impact of  
315 the contrast of year on CDD index is significant over the west and central Sahel for both wet  
316 and dry experiments. However, the strongest impact of the contrast of year is found in wet  
317 experiments over the central Sahel reached 4 days (Fig.7a). The impact on CDD index in the  
318 dry year is strong than wet year.

319 **In summary, RegCM4 overestimates the maximum number of consecutive dry days over most**  
320 **of the domain studied, except over the Guinea coast. The strongest linear impact on the CDD**

321 index for the dry (wet) experiments is found over the west Sahel with a peak around -6 days  
322 (2 days). The maximum number of consecutive dry days is sensitive to the contrast of year  
323 over the west and central Sahel.

324

### 325 **3.1.4 The maximum number of consecutive wet days (CWD index).**

326 The persistence of wet spells (CWD index) which represents the maximum number of  
327 consecutive wet days with precipitation  $\geq 1 \text{ mm.day}^{-1}$  is investigated in this section. Figure 8  
328 (first panel) is the same as Fig.2 (first panel) but shows the maximum number of consecutive  
329 wet days (CWD index, in day). The observation products TRMM (Fig.8b, e) and CHIRPS  
330 (Fig.8a, d) depict a similar large-scale pattern with the PCCs reached 0.90 and 0.87 (resp. for  
331 JJAS 2003 and JJAS 2004, Table 2). CHIRPS observation located the maximum of CWD  
332 index over the mountain regions such as Cameroon mountains, Jos plateau and Guinea  
333 highlands and it is more than 20 days. While the minimum values of CWD index are found  
334 over most of the area above the latitude  $17^{\circ}\text{N}$  and not exceed 4 days (Fig.8a, d). In general,  
335 the differences between TRMM and CHIRPS observation concern the maxima magnitude and  
336 its extent, which are more pronounced in TRMM than CHIRPS. Generally, TRMM  
337 underestimates the CWD index over most of the domains studied compared to CHIRPS. The  
338 largest mean bias is found over the Guinea coast region with MB more than 2.47 and 2.38  
339 days (resp. for JJAS 2003 and JJAS 2004, Table 2).

340 The control experiments well reproduce the large-scale pattern over the entire West African  
341 domain, with PCCs values about 0.81 and 0.87 (resp. for JJAS 2003 and JJAS 2004, Table 2).  
342 However, at the local scale the control experiments exhibit some biases in maxima and  
343 minima CWD index values in term of magnitude and spatial extent. Control experiments  
344 overestimate the CDD index over the different domains studied (Fig. 8 c, f). We noted that,  
345 this overestimation area coincides with the excessive values of R1mm index (Fig.2c, f). The  
346 strongest mean bias is found over the Guinea coast, more than 59.21 and 60.51 days (resp. for  
347 JJAS 2003 and JJAS 2004).

348 Figure 8 (second panel) is the same as Fig.2 (second panel), but displays changes in CWD  
349 index. As for R1mm index, over the central Sahel, the impact is linear, the dry (wet)  
350 experiments tends to decrease (increase) the maximum number of consecutive wet days  
351 (CWD index) for wet and dry years (resp JJAS 2003 and JJAS 2004). This result confirms the  
352 strong soil moisture impact over the transition zones with a climate between dry and wet  
353 regimes (Zhang et al., 2011; Koster et al., 2006). However, over Guinea and the west Sahel,

354 the changes are not linear, both dry and wet experiments lead to cause an increase, in JJAS  
355 2003 and JJAS 2004 (Fig. 8B, c).

356 Figure 9, as in Fig.3, but shows the PDF distribution of changes in CWD index. The impact  
357 on CWD index found over the central Sahel are linear. The dry (wet) experiments tend to  
358 decrease (increase) the CWD index with peaks at -10 days (15 days) for both JJAS 2003 and  
359 JJAS 2004. However, for the other sub-regions studied, particularly over the Guinea coast,  
360 wet and dry experiments tend to increase the CWD index, with peaks 10 and 2 days  
361 respectively (Fig. 9c). The CWD index is not sensitive to the contrast of the year over the  
362 different domains studied (Fig 9).

363 Summarizing the results of this section, as in R1mm and CDD indices, the CWD index is only  
364 linear over the central Sahel, the dry (wet) experiments tends to decrease (increase) of the  
365 CWD index. The model RegCM4 overestimates the duration of wet days over all the domains  
366 studied. This overestimation is linked with an excessive number of wet days as documented  
367 by Diaconescu et al. (2014).

368

### 369 **3.1.5 The maximum one-day precipitation accumulation (RX1day index).**

370 The maximum one-day precipitation accumulation during the period JJAS 2003 and JJAS  
371 2004 is assessed in this section. Figure 10 (first panel) is the same as Figure 2 (first panel), but  
372 shows the spatial distribution of the RX1day index. The observations datasets TRMM  
373 (Fig.10b, e) and CHIRPS (Fig.10 a, d) present quite differences in term of the spatial extent of  
374 the maximum values of RX1day index, although their large-scale pattern is similar with PCC  
375 more than 0.84 for both JJAS 2003 and JJAS 2004 (Table 2). Over the Guinea and Sahel  
376 regions, the spatial extends of RX1day index maxima values more than 80 mm is large on  
377 TRMM, while CHIRPS datasets they are confined over the coastline of the Gulf of Guinea.  
378 TRMM observation overestimates the maximum one-day precipitation accumulation over the  
379 entire domain studied compared to CHIRPS. The largest maximum one-day precipitation is  
380 found over the central Sahel with MB reached 35.78 and 31.66 (resp. for JJAS 2003 and JJAS  
381 2004, Table 2).

382 The control experiments capture the spatial pattern with PCC values 0.50 and 0.4 (resp. JJAS  
383 2003 and JJAS 2004, Table2). This low coefficient of PCC has been also obtained by Thanh  
384 et al. (2017) over Asia with RegCM4 (correlation <0.3). The model simulations failed to  
385 capture the magnitude and the spatial extent of RX1day index maxima values. The control  
386 experiments underestimate the RX1day index over all the domains studied. The RX1day

387 index is underestimated over the entire domain studied, this is also due to the excessive light  
388 precipitation, simulated by the current physical parameterization of RegCM4. The largest  
389 underestimation is located over the Guinea coast and the west Sahel. For instance, over the  
390 west Sahel, the MB is about -38.07 and -36.67 mm (resp. JJAS 2003 and JJAS 2004, Table  
391 2).

392 Figure 10 (second panel) is similar to Fig. 2 (second panel), but displays changes in maximum  
393 one-day precipitation. As for SDII index, the initial soil moisture anomalies impact on the  
394 RX1day index is not linear, a similar mixture of increase and decrease of RX1day index is  
395 shown for dry and wet experiments over most of the domains studied (Figure 10 second  
396 panel).

397 Figure 11, as in Fig.3, but shows the PDF distribution of changes in RX1day index. The  
398 impact of the contrast of years on RX1day index is significant, only over the west Sahel in  
399 wet experiments about 7 mm.

400 In summary, RegCM4 underestimates the maximum one-day precipitation accumulation over  
401 the entire domain studied. A non-linear trend is identified over the different domains studied.  
402 As for SDII index, RX1day index is related to precipitation intensity and the impact of wet  
403 and dry experiments on the maximum one-day precipitation accumulation is not significant.  
404 The maximum one-day precipitation accumulation is sensitive to the contrast of years,  
405 especially over the west Sahel in wet experiments.

406

### 407 **3.1.6 Precipitation percent due to very heavy precipitation days (R95pTOT index)**

408 We investigated in this section, the precipitation percent due to very heavy precipitation days  
409 during the period JJAS 2003 and JJAS 2004. Figure 12 (first panel) is the same as Fig.2 (first  
410 panel), but shows the spatial distribution of R95pTOT index. TRMM (Fig.12b, e) and  
411 CHIRPS observations (Fig.12a, d) present a similar spatial pattern over the entire West  
412 African domain with PCC value reached 0.91 for both JJAS 2003 and JJAS 2004 (Table 2).  
413 However, some biases are noticed for R95pTOT index maxima in term of spatial extent. As  
414 for RX1day index, TRMM observation extends maxima of R95pTOT index more than 60 %  
415 over the Guinea and the Sahel region (Fig.10), while CHIRPS confine them over the Guinea  
416 coast. Overall, TRMM shows a dominant overestimation than CHIRPS over the West African  
417 domain about 16.54 and 18.54 % (resp. JJAS 2003 and JJAS 2004, Table2). The control  
418 experiments (Fig.12c, f) capture the spatial pattern with PCC values 0.59 and 0.55 (resp. JJAS  
419 2003 and JJAS 2004, Table2). As with SDII and RX1day indices, the control experiments

420 underestimate the values of the R95pTOT index, while they overestimated the R1mm index.  
421 This is also due by the current physical parameterization scheme of the RegCM4 model which  
422 results in a positive bias for the number of wet days with a low precipitation threshold (e. g. 1  
423 mm.day<sup>-1</sup>), while results in negative bias for the indices of the number of wet days with a  
424 higher precipitation threshold (e. g. 10 mm.day<sup>-1</sup>, not shown here). The control experiments  
425 underestimate the R95pTOT index over the different domains studied. The largest  
426 underestimation of R95pTOT index is located over the Guinea coast with MB more than - 43  
427 and - 46 % (resp. for JJAS 2003 and JJAS 2004, Table2).

428 Figure 12 (second panel) is similar to Fig.2 (second panel), but displays changes in R95pTOT  
429 index. Both dry and wet experiments tend to cause an increase of R95pTOT index over the  
430 orographic regions. This means that the initial soil moisture conditions, whether dry or wet,  
431 tend to reinforce extreme floods.

432 Figure 13 is the same as Fig.3, but shows the PDF distribution of changes in R95pTOT index.  
433 An increasing in R95pTOT index for both wet and dry experiments is shown over most of the  
434 domains studied. The largest change is found over the west Sahel with the peak around 5 %  
435 and 2 % respectively for wet and dry experiments (Fig.13 b). The impact of the contrast of the  
436 wet and dry years on R95pTOT index is significant about reached 2 % (resp. JJAS 2003 and  
437 JJAS 2004), especially over west Sahel (Fig. 13a). The impact on R95pTOT index in the wet  
438 year is strong over the different domains studied compared to dry year.

439 In summary, RegCM4 underestimates the precipitation percent due to very heavy  
440 precipitation days over the West African domain. The initial soil moisture conditions, whether  
441 dry or wet, tend to accentuate the precipitation percent due to very heavy precipitation days.  
442 This result is in line with Liu et al. (2014) work over Asia using RegCM4. The precipitation  
443 percent due to very heavy precipitation days is sensitive to the contrast of years over the west  
444 Sahel in the wet experiments.

445

### 446 **3.2. Seasonal temperature extreme indices**

447 In this section, using daily maximum and minimum temperature, we analyze four extreme  
448 temperature indices (Table 1) in RegCM4 simulations over West Africa. All temperature  
449 indices are calculated for JJAS 2003 and JJAS 2004. Table 3 summarizes the pattern  
450 correlation coefficient (PCC) and the mean bias (MB) of all temperature indices studied in  
451 this section for EIN reanalysis and model simulations derived from control experiments with



452 initial soil moisture from ERA20C reanalysis, with respect to GTS observation, calculated  
453 over the domains presented in Fig 1, during the period JJAS 2003 and JJAS 2004.

454

### 455 **3.2.1. Maximum value of daily maximum temperature (TXx index)**

456 In this section, we analyzed the TXx index which gives the hottest day's temperature during  
457 JJAS 2003 and JJAS 2004. Figure 14 (first panel) shows TXx index in °C) from GTS  
458 observation (Fig.14a, d) and EIN reanalysis (Fig.14b, e) for JJAS 2003 and JJAS 2004 and  
459 their corresponding simulated control experiments (Fig.14c, f) with the initial soil moisture of  
460 the reanalysis ERA20C. The GTS observation shows the highest values of the TXx index  
461 observed over the Sahara, more than 46° C. While the lowest values (less than 32°C) are  
462 found over the Guinea coast (Fig.14a, d). The EIN reanalysis have similar large-scale patterns  
463 with PCC value 0.99 over the entire West African domain (Table 3). However, some biases  
464 are shown at the local scale in terms of magnitude and spatial extent of these maxima and  
465 minima. The reanalysis of the EIN (Fig.14b, e) shows lower values (less than 28°C) of the  
466 TXx index over a large area along the Guinea coastline compared to GTS datasets.  
467 Conversely, GTS observation presents higher values of TXx index (up to 48°C) over a large  
468 area as compared to EIN reanalysis. The reanalysis of the EIN shows a negative bias of the  
469 TXx index over most of the domains studied (Table 3).

470 The control experiments (Fig.14c, f) reasonably well replicate the large-scale patterns of TXx  
471 index values with PCCs up to 0.99 over the entire West African domain, but they exhibit  
472 some biases a local scale. The control experiments are closer to the maximum and minimum  
473 values display in GTS observation. The control simulations overestimate the TXx values over  
474 the central and west Sahel and over the Guinea coast they are underestimated (Table 3). For  
475 instance, the greatest overestimation is found over the west Sahel with MB about 3.02 and  
476 2.02°C (resp. for JJAS 2003 and JJAS 2004, Table3). However, these biases obtained for TXx  
477 index in this study are much lower compared to Thanh et al. (2017) work using RegCM4 over  
478 the Asia where it reached 8° C.

479 Figure 14 (second panel) displays changes in TXx index for JJAS 2003 and JJAS 2004, for  
480 dry (Fig.14g, i, resp. for JJAS 2003 and JJAS 2004) and wet experiments (Fig.14h, j, resp.  
481 for JJAS 2003 and JJAS 2004) with respect to their corresponding control experiments, the  
482 dotted area shows changes with statistical significance of 10% level. The impact of the initial  
483 soil moisture conditions on TXx index is linear over the entire West African domain, i.e. the  
484 dry experiments lead to an increase of TXx index values while the wet experiments favor a

485 decrease of TXx index values. We noted that this linear impact is more pronounced in dry and  
486 the wet experiments over the Guinea coast and the central Sahel respectively (Fig.14, second  
487 panel).

488 The PDF distributions of TXx index changes for JJAS 2003 and JJAS 2004, over (a) the  
489 central Sahel, (b) West Sahel, (c) Guinea and (d) West Africa derived from dry and wet  
490 experiments compared to the corresponding control experiments are shown in Figure 15. As  
491 mentioned, the results confirm the linear impact on TXx index of the initial soil moisture  
492 conditions over all the domains studied. The strongest impact is found over the central Sahel  
493 (Fig.15a) with a decrease (increase) of TXx index and the peak is around  $-2.5^{\circ}\text{C}$  (more than  
494  $1^{\circ}\text{C}$ ) in wet (dry) experiments. The impact of the contrast years on TXx index is found  
495 particularly in dry experiments over the central Sahel reached  $0.8^{\circ}\text{C}$  (Fig.15a). The impact of  
496 the dry year (JJAS 2004) is strong than the wet year (JJAS 2003).

497 In summarizing this section, during the JJAS 2003 and 2004, the model RegCM4  
498 overestimates and underestimates the hottest day's temperature respectively over the Sahel  
499 (west and central) and Guinea coast. The impact on TXx index is linear over all the different  
500 domains studied, i.e. the dry (wet) experiments decrease (increase) the TXx index. The TXx  
501 index is sensitive to the contrast of year, particularly in dry experiments over the central  
502 Sahel.

503

### 504 **3.2.2. The Minimum value of daily maximum temperature (TXn index).**

505 In this section, we investigated the TXn index which gives the lowest day's temperature  
506 during JJAS 2003 and JJAS 2004. Figure 16 (first panel) is the same as Fig.14 (first panel)  
507 but presents the spatial distribution of the TXn index. GTS observation (Fig.16a, d) and EIN  
508 reanalysis (Fig.16b, e) display similar features with PCC reached 0.99 (for JJAS 2003 and  
509 JJAS 2004, Table 3). The maxima and minima values of TXn index are located over the  
510 Sahara and the Guinea coast respectively. However, there are some differences at the local  
511 scale in terms of spatial extent and magnitude. The EIN reanalysis presents a larger spatial  
512 extent of the maxima (greater than  $36^{\circ}\text{C}$ ) and minima (less than  $24^{\circ}\text{C}$ ) compared to GTS  
513 observation. The EIN reanalysis show a negative bias value over Guinea coast and west Sahel  
514 (for both JJAS 2003 and JJAS 2004 Table3). For instance, over the Guinea coast with MB  
515 about  $-0.70$  and  $-1.38^{\circ}\text{C}$  (resp. for JJAS 2003 and JJAS 2004, Table 3).

516 The control experiments show a good agreement with the GTS datasets in the large scale  
517 patterns with PCC about 0.99, however, the magnitude of the TXn index over all the domains

518 studied are overestimated. For instance, over the West African domain, the MB is about 5.65  
519 and 4.14°C (resp. JJAS 2003 and JJAS 2004, Table 3). The biases obtained in this study are  
520 lower compared to a similar study carried out by Thanh et al. (2017) over Asia using  
521 RegCM4,

522 As for Fig.14 (second panel), the Figure 16 (second panel) displays changes in TXn index.  
523 The impact on TXn index of the initial soil moisture anomalies are linear over the entire West  
524 African domain, i.e. the dry experiments lead to an increase of TXn index values while the  
525 wet experiments favor a decrease of TXn index values. The strongest impact on TXn index is  
526 found in wet experiments above the latitude 15 °N, especially for JJAS 2003.

527 Figure 17 is the same as Fig.15 but displays the PDF distribution of changes in TXn index.  
528 The impact on TXn index of initial soil moisture conditions is linear over most of the domain  
529 studied, although this impact is rather weak as compared to the TXx index. The strongest  
530 impact on TXn index for wet experiments are found over the wet Sahel about -2°C, while in  
531 dry experiments, it is found over the central Sahel not exceed 1° C. Moreover, the changes in  
532 TXn index are sensitive to the contrast of year, especially in dry experiments over west Sahel  
533 reached 0.8°C (Fig. 13b). The impact on TXn index in the dry year is strong than the wet year  
534 over the west Sahel.

535 In summary, RegCM4 overestimates the lowest day's temperature during JJAS 2003 and JJAS  
536 2004 over the whole West African domain. As for TXx index, the impact on TXn index to  
537 soil moisture anomalies is linear, i.e. the dry (wet) experiments tend to cause an increase  
538 (decrease) of TXn index values over most of the domain studied. The impact on TXn index  
539 of the initial soil moisture conditions is low compared to the TXx index. The TXn index is  
540 sensitive to the contrast of year, especially in dry experiments over west Sahel.

541

### 542 3.2.3. The Minimum value of daily minimum temperature (TNn index).

543 In this section, we examined the TNn index which gives the lowest temperature at night  
544 during JJAS 2003 and JJAS 2004. Figure 18 (first panel) is the same as Fig.14 (first panel)  
545 but displays the spatial distribution of the TNn index. GTS observation (Fig.18 a, d) shows  
546 the maxima of TNn index values above the latitude 15° N not exceeding 27° C, while the  
547 minima values are less than 17°C and located over the mountain regions such as Cameroon  
548 mountain, Jos Plateau and Guinea Highland. The EIN reanalysis shows a similar spatial  
549 pattern with GTS observation, with PCC value about 0.99 over the whole West African  
550 domain (Table 3) despite some biases at the local scale. The EIN reanalysis (Fig.18 b, e)

551 displays the highest value of TNn index (exceeding 27°C) than GTS observation and they are  
552 located over a large area above the latitude 15° N. The EIN reanalysis also shows the lowest  
553 values (less than 21°C) of TNn index than GTS observation, located over the orographic  
554 regions. The EIN reanalysis overestimates the TNn index values over most of the domain  
555 studied. For instance, over the West African domain, the MB reaches 3.15 and 3.11°C (resp.  
556 for JJAS 2003 and JJAS 2004, Table 3).

557 The control experiments (Fig.18 c, f) show a good agreement with GTS observation with PCC  
558 values about 0.99 but do exhibit some biases at the local scale. The control experiments  
559 overestimate the magnitude of the TNn index over all the domains studied. For instance, over  
560 the West African domain, the MB is about 1.45 °C and 0.71°C (resp. for JJAS 2003 and JJAS  
561 2004, Table 3). These positive biases obtained in simulating the TXx, TXn and TNn indices  
562 are opposite with the cold bias known with RegCM4 in mean climate simulation (Koné et al.,  
563 2018, Klutse et al., 2016). It is very difficult to know the origin of RCM temperature biases,  
564 as they can depend on several factors, such as surface energy fluxes and water, cloudiness,  
565 surface albedo (Sylla et al., 2012; Tadross et al., 2006).

566 Figure 18 (second panel) is the same as Fig.14 (second panel), but displays changes in TNn  
567 index. The impact on TNn index of the initial soil moisture conditions is linear over the  
568 Sahara region, i.e. the wet experiments lead to an increase of TNn index values while the dry  
569 experiments favor a decrease of TNn index values. We noticed this linear impact coincides  
570 with the area of highest TNn index values over the Sahara (Fig.18, first panel). However, over  
571 the central and west Sahel, both dry and wet experiments lead to a decrease. Conversely, over  
572 the Guinea coast, we found an increase.

573 Figure 19 is the same as Fig.15 but shows the PDF distribution of changes in TNn index. The  
574 impact on changes in TNn index, are not linear over all the domains studied. However,  
575 although this impact is weak, over central and west Sahel it tends to decrease, while over the  
576 Guinea coast it increases. The strongest impact is found over the west Sahel, where the wet  
577 and dry experiments lead to a decrease in TNn index, with the peaks around - 1°C and - 0.2°C  
578 respectively. The impact of the contrast years on TNn index is not significant over all the  
579 different domains studied.

580 **In summary, RegCM4 overestimates the lowest temperature at night during JJAS 2003 and**  
581 **JJAS 2004 over the different domains studied. The impact on TNn index of the soil moisture**

582 conditions is linear only over the Sahara, i.e. the dry (wet) experiments tend to decrease  
583 (increase) the TNn index values. The TNn index is not sensitive to contrast years.

584

### 585 **3.2.4. The Maximum value of daily minimum temperature (TNx index)**

586 In this section, we turned our attention to TNx index which gives the warmest night  
587 temperature during JJAS 2003 and JJAS 2004. Figure 20 (first panel) is the same as Fig.14  
588 (first panel), but for TNx index. GTS observation (Fig.20 a, d) shows the maxima of TNx  
589 index values over the Sahara reached 40° C, while the minima values around 24°C are located  
590 over the Guinea coast sub-region. The EIN reanalysis (Fig.20 b, e) shows similar large scale  
591 patterns with PCC value reached 0.99, but some biases can be noticed between GTS and EIN  
592 datasets. The EIN reanalysis underestimates the maxima (not exceeds 38°C) and the minima  
593 (less than 22°C) located respectively over the Sahara and the orographic regions such as  
594 Cameroon mountains, Jos plateau and Guinea highlands. The strongest negative mean bias is  
595 located over the Guinea coast with MB about -3.11°C and -3.14°C (resp. JJAS 2003 and JJAS  
596 2004, Table 3).

597 The control experiments (Fig.20 c, f) well reproduce the general features of TNx index with a  
598 PCC value reached 0.99 but some differences are shown at the local scale. Unlike the TNN  
599 index, the control experiments underestimate the TNx index, over most of the domains  
600 studied. The maxima of TNx index values are quite underestimated over the Sahara. For  
601 instance, over the central Sahel, the MB is about -3.85°C and -3.99°C (resp. for JJAS 2003  
602 and JJAS 2004, Table 3). This underestimation of TNx index seems to be systematic related  
603 to the cold bias in RegCM4 over West Africa which is shown by several papers (Koné et al.,  
604 2018, Klutse et al., 2016).

605 Figure 20 (second panel) is the same as Fig.14 but displays changes in TNx index, as in  
606 Fig.14 (second panel). As for TNn index, the impact on TNx index of initial soil moisture  
607 conditions is somewhat linear over the Sahara, i.e. the dry experiments lead to an increase of  
608 TNx index values while the wet experiments favor a decrease of TNx index values. However,  
609 over the central and west Sahel, although the signal is weak, both wet and dry experiments  
610 lead to a dominant decrease. Conversely, over the Guinea coast, the impact on TNx index  
611 leads to a dominant increase.

612 Figure 21 is the same as Fig.15, but displays the PDF distributions of the changes in TNx  
613 index. As for TNn index, the impact on TNx index changes is not linear over the different  
614 domains studied. We noticed that TNx index is more sensitive to the wet and dry experiments

615 over the central Sahel than the other sub-regions studied. The strongest impact in the wet  
616 experiments is found over the central Sahel (Fig. 21 a) and it's about  $-1.3^{\circ}\text{C}$ , while in dry  
617 experiments it's found over the west Sahel and it is more than  $-1^{\circ}\text{C}$  (Fig. 21 b). The sensitivity  
618 of TNx index to the contrast of years is significant over the central Sahel about  $-1^{\circ}\text{C}$  In wet  
619 experiments.

620 In summary, RegCM4 underestimates the warmest night temperature during JJAS 2003 and  
621 JJAS 2004 over the different domains studied. As for TNn index, the impact on TNx index of  
622 the initial soil moisture conditions is linear only over the Sahara, i.e. the dry (wet)  
623 experiments tend to decrease (increase) the TNn index values. The impact on TNx index of  
624 initial soil moisture conditions is greater compared to TNn index, The TNx index is sensitive  
625 to the contrast years over central Sahel in wet experiments

#### 626 4. Conclusions

627 The impact on the subsequent summer extreme climate of the initial soil moisture conditions  
628 over West Africa is investigated using the RegCM4-CLM45. In addition, the performance of  
629 RegCM4-CLM4.5 in representing six extreme indices of precipitation and four extreme  
630 indices of temperature over West Africa was also evaluated. Results have been presented for  
631 JJAS 2003 (wet year) and JJAS 2004 (dry year). We performed sensitivity studies over the  
632 West African domain, with 25 km of spatial resolution. We initialized the control runs by  
633 ERA20C reanalysis soil moisture, and at its wilting points and the field capacity respectively  
634 for dry and wet experiments.

635 Compared to the extreme indices of the observation datasets, the model overestimated and  
636 underestimated the number of the wet days respectively for a low ( $1\text{mm}\cdot\text{day}^{-1}$ ) and high  
637 threshold rain rate (e.g.  $10\text{ mm}\cdot\text{day}^{-1}$ , not shown here). RegCM4 also underestimates the  
638 simple precipitation intensity index (SDII index), the maximum 1-day precipitation (Rx1day  
639 index) and the precipitation percent due to very heavy precipitation days (R95pTOT index).  
640 The current physical parameterization scheme of the RegCM4 model used in our study results  
641 in a positive bias for the number of wet days with a low precipitation threshold (e. g.  
642  $1\text{mm}\cdot\text{day}^{-1}$ ), while in a negative bias for a higher precipitation threshold (e.g.  $10\text{ mm}\cdot\text{day}^{-1}$ ,  
643 not shown here). However, RegCM4 generally overestimates the maximum number of  
644 consecutive wet and dry days (resp. CWD and CDD indices) over the West African domain  
645 studied. For the temperature extreme indices used in this study (TXx, TXn and TNn) are also  
646 overestimated, except TNx index, which is underestimated over the West African domain.



647 The impact on extreme precipitation indices of the initial soil moisture conditions is linear  
648 only for indices related to the number of precipitation events (R1mm, CDD and CWD  
649 indices), and not for those related to the amount of precipitation (SDII, RX1day and  
650 R95pTOT). The dry and wet experiments accentuate the precipitation percent due to very  
651 heavy precipitation days (R95pTOT index) over most of the domain studied. In addition,  
652 among all the precipitation indices studied, the contrast of years impacts significantly only the  
653 CDD index on the central Sahel in particular for wet experiments.

654 Generally, the impact on extreme temperatures of the initial soil moisture conditions is great  
655 compared to extreme precipitation. Overall, the initial soil moisture conditions unequally  
656 affect the daily maximum and minimum temperature over the West African domain. There is  
657 a greater impact on daily maximum temperature extremes than on the daily minimum  
658 temperature extremes. These results are in line with previous works (Jaeger and Seneviratne,  
659 2011; Zhang et al., 2009).

660 The wet (dry) experiments result in an increase (decrease) in the TXx and TXn indices over  
661 most of the areas studied. The impact of initial soil moisture conditions on the indices related  
662 to the minimum temperature (TNx and TNn indices) is not linear over most of the domains  
663 studied. The strongest impact on minimum temperature indices (TNn and TNx indices) is  
664 somewhat linear over the Sahara. The dry (wet) experiments tend to cause an increase (a  
665 decrease) in the TNn and TNx indices over the Sahara.

666 This study helps to understand the impact of the initial soil moisture conditions on extreme  
667 events of precipitation and temperature in terms of intensity and duration over West Africa. It  
668 is a contribution to the improvement of extreme events forecasts in West Africa in  
669 highlighting the crucial role of initial soil moisture. For a proper assessment of the  
670 dependence of the model in our results, it would be appropriate to repeat the investigation  
671 using different RCMs in a multi-model framework.

672

### 673 **Author contribution**

674 The authors declare to have no conflict of interest with this work. B. Koné and A. Diedhiou  
675 fixed the analysis framework. B. Koné carried out all the simulations and figures production  
676 according to the outline proposed by A. Diedhiou. B. Koné and A. Diedhiou, S. Anquetin and  
677 A. Diawara worked on the analyses. All authors contributed to the drafting of this manuscript.

678

679 **Acknowledgements**

680 The research leading to this publication is co-funded by the NERC/DFID “Future Climate for  
681 Africa” programme under the AMMA-2050 project, grant number NE/M019969/1 and by  
682 IRD (Institut de Recherche pour le Développement; France) grant number UMR IGE  
683 Imputation 252RA5.

684

685 **References:**

686

687 Bichet, A., & Diedhiou, A. (2018a). West African Sahel has become wetter during the last 30  
688 years, but dry spells are shorter and more frequent. *Climate Research*, 75(2), 155-162.

689

690 Bichet, A., & Diedhiou, A. (2018b). Less frequent and more intense rainfall along the coast of  
691 the Gulf of Guinea in West and Central Africa (1981–2014). *Climate Research*, 76(3), 191-  
692 201.

693

694 Danielson J.J., and Gesch D.B.: Global multi-resolution terrain elevation data 2010  
695 (GMTED2010): U.S. Geological Survey Open-File Report 2011–1073, 26 p, 2011.

696

697 Didi Sacré Regis M , Mouhamed, L., Kouakou, K., Adeline, B., Arona, D., Koffi Claude A,  
698 K., ... & Issiaka, S. (2020). Using the CHIRPS Dataset to Investigate Historical Changes in  
699 Precipitation Extremes in West Africa. *Climate*, 8(7), 84.

700

701 Dee D. P., Uppala S. M., Simmons A. J., Berrisford P., Poli P., Kobayashi S., Andrae U.,  
702 Balmaseda, M. A., Balsamo G., Bauer, P., Bechtold P., Beljaars A. C. M., van de Berg L.,  
703 Bidlot J., Bormann N., Delsol C., Dragani R., Fuentes M., Geer A. J., Haimberger L., Healy  
704 S. B., Hersbach H., Hólm E. V., Isaksen L., Kållberg P., Köhler M., Matricardi M., McNally  
705 A. P., Monge-Sanz B. M., Morcrette J.-J., Park, B.-K., Peubey C., de Rosnay P., Tavolat C.,  
706 Thépaut J.-N. and Vitart F.: The ERA-Interim reanalysis: configuration and performance of  
707 the data assimilation system, *Q. J. Roy. Meteorol. Soc.*, 137, 553-597,  
708 <https://doi.org/10.1002/qj.828>, 2011.

709

710 Diaconescu E. P., Gachon P. , Scinocca J., and LapriseR.: Evaluation of daily precipitation  
711 statistics and monsoon onset/retreat over western Sahel in multiple data sets. *Climate Dyn.*,  
712 45, 1325–1354, doi:10.1007/s00382-014-2383-2, 2015 .  
713

714 Easterling, D.R., Meehl, G.A., Parmesan, C., Changnon, S.A., Karl, T.R. and Mearns, L.O.:  
715 Climate Extremes: Observations, Modeling and Impacts. *Science* , 289, 2068-2074.  
716 <https://doi.org/10.1126/science.289.5487.2068>, 2000.  
717

718 Emanuel K. A.: A scheme for representing cumulus convection in large-scale models. *Journal*  
719 *of the Atmospheric Science* 48: 2313–2335, 1991.  
720

721 Fan Y., and van den Dool H. : A global monthly land surface air temperature analysis for  
722 1948 -present, *J. Geophys. Res.* 113, D01103, doi: 10.1029/2007JD008470, 2008.  
723

724 Folland C. K., Palmer T. N. , and Parker D. E.: Sahel rainfall and worldwide sea  
725 temperatures, *Nature*, 320, 602 – 607, 1986.  
726

727 Fontaine B., Janicot S. , and Moron V. : Rainfall anomaly patterns and wind field signals over  
728 West Africa in August (1958 – 1989), *J. Clim.*, 8, 1503 –1510, 1995.  
729

730 Giorgi F., Coppola E., Solmon F., Mariotti L., Sylla M. B., Bi X., Elguindi N., Diro G. T.,  
731 Nair V., Giuliani G., Cozzini S., Guettler I., O’Brien T., Tawfik A., Shalaby A., Zakey A. S.,  
732 Steiner A., Stordal F., Sloan L., and Brankovic C. : RegCM4: model description and  
733 preliminary tests over multiple CORDEX domains, *Clim. Res.*, 52, 7–29,  
734 [doi.org/10.3354/cr01018](https://doi.org/10.3354/cr01018), 2012.  
735

736 Grell G., Dudhia J. and Stauffer D. R.: A description of the fifth generation Penn State/NCAR  
737 Mesoscale Model (MM5), National Center for Atmospheric Research Tech Note NCAR/TN-  
738 398+STR, NCAR, Boulder, CO, 1994.  
739

740 Holtslag A., De Bruijn E., and Pan H. L. : A high resolution air mass transformation model  
741 for short-range weather forecasting, *Mon. Weather Rev.*, 118, 1561–1575, 1990.

742  
743 Hong S. Y. and Pan H. L.: Impact of soil moisture anomalies on seasonal, summertime  
744 circulation over North America in a regional climate model. *J. Geophys. Res.*, 105 (D24), 29  
745 625–29 634, 2000.  
746  
747 Huffman, G. J., Adler, R. F., Bolvin, D. T., Gu, G., Nelkin, E. J., Bowman, K. P., Hong, Y.,  
748 Stocker, E. F., and Wolff, D. B.: The TRMM multisatellite precipitation analysis: quasi-  
749 global, multiyear, combined-sensor precipitation estimates at fine scale, *J. Hydrometeorol.*, 8,  
750 38–55, 2007.  
751  
752 Jaeger E. B., and Seneviratne S. I. : Impact of soil moisture-atmosphere coupling on  
753 European climate extremes and trends in a regional climate model, *Clim. Dyn.*, 36(9-10),  
754 1919-1939, doi:10.1007/s00382-010-0780-8, 2011.  
755  
756 Kang S, Im E.-S. and Ahn J.-B.: The impact of two land-surface schemes on the  
757 characteristics of summer precipitation over East Asia from the RegCM4 simulations *Int. J.*  
758 *Climatol.* 34: 3986–3997, 2014.  
759  
760 Kim J-E., and Hong S-Y.: Impact of Soil Moisture Anomalies on Summer Rainfall over East  
761 Asia: A Regional Climate Model Study, *Journal of Climate*. Vol. 20, 5732–5743, DOI:  
762 10.1175/2006JCLI1358.1, 2006.  
763  
764 Kiehl J. T., Hack J. J., Bonan G. B., Boville, B. A., Briegleb B. P., Williamson D. L., and  
765 Rasch P. J.: Description of the NCAR Community Climate Model (CCM3), Technical Note  
766 NCAR/TN–420+STR, 152, 1996.  
767  
768 Koné B., Diedhiou A., N’datchoh E. T., Sylla M. B. , Giorgi F., Anquetin S., Bamba A.,  
769 Diawara A., and Koba A. T.: Sensitivity study of the regional climate model RegCM4 to  
770 different convective schemes over West Africa. *Earth Syst. Dynam.*, 9, 1261–1278.  
771 <https://doi.org/10.5194/esd-9-1261-2018>, 2018.  
772  
773

774 Koster R. D., GUO Z. H., Dirmeyer P. A., Bonan G., Chan E., Cox P., Davies H., Gordon C.  
775 T., Gordon C. T., Lawrence D., Liu P., Lu C. H, Malyshev S., McAvaney B., Mitchell K,  
776 Mocko D., Oki K., Oleson K., Pitman A., Sud Y. C. , Taylor C. M., 16 Versegny D., Vasic  
777 R., Xue Y., Yamada T.: The global land–atmosphere coupling experiment. Part I: Overview,  
778 *J. Hydrometeorol.*, 7(4), 590–610, doi:10.1175/JHM510.1, 2006.

779

780 Larsen J.: Record heat wave in Europe takes 35,000 lives. Earth Policy Institute, 2003.

781

782 Le Barbé L., Lebel L., and Tapsoba D.: Rainfall variability in west africa during the years  
783 1950-1990. *J. Climate*, 15 :187–202., 2002.

784

785 Loveland TR, Reed BC, Brown JF, Ohlen DO, Zhu Z, Yang L, J. W. Merchant J. W.:  
786 Development of a global land cover characteristics database and IGBP DISCover from 1km  
787 AVHRR data. *International Journal of Remote Sensing* 21: 1303–1330, 2000.

788

789 Liu D., G. Wang R. Mei Z. Yu, and Yu M. : Impact of initial soil moisture anomalies on  
790 climate mean and extremes over Asia, *J. Geophys. Res. Atmos.*, 119, 529–545,  
791 doi:10.1002/2013JD020890, 2014.

792

793 Klutse B. A. N., Sylla B. M., Diallo I., Sarr A., Dosio A., Diedhiou A., Kamga A., Lamptey  
794 B., Ali A., Gbobaniyi E. O., Owusu K., Lennard C., Hewitson B., Nikulin G., & Panitz H.-J.,  
795 Büchner M.: Daily characteristics of West African summer monsoon precipitation in  
796 CORDEX simulations. *Theor Appl Climatol.* 123:369–386 DOI 10.1007/s00704-014-1352-3,  
797 2016.

798

799 Nicholson, SE.: The nature of rainfall fluctuations in subtropical West-Africa. *Mon. Wea.*  
800 *Rev.* 22109, 2191-2208, 1980.

801

802 Nicholson SE.: Land Surface processes and Sahel climate. *Reviews of Geophysics.* 38(1),  
803 117-24139, 2000.

804

805 Nikulin G., Jones C., Samuelsson P., Giorgi F., Asrar G., Büchner M., Cerezo-Mota R.,  
806 Christensen O. B., Déque M., Fernandez J., Hansler A., van Meijgaard E., Sylla M. B. and  
807 Sushama L.: Precipitation climatology in an ensemble of CORDEX-Africa regional climate  
808 simulations, *J. Climate*, 6057–6078, <https://doi.org/10.1175/JCLI-D-11-00375.1>, 2012.  
809

810 Oleson K., Lawrence D. M., Bonan G. B., Drewniak B., Huang M., Koven C. D., Yang Z.-L.:  
811 Technical description of version 4.5 of the Community Land Model (CLM) (No. NCAR/TN-  
812 503+STR). doi:10.5065/D6RR1W7M, 2013.  
813

814 Pal J. S., Small E. E. and Elthair E. A.: Simulation of regional scale water and energy  
815 budgets: representation of subgrid cloud and precipitation processes within RegCM, *J.*  
816 *Geophys. Res.*, 105, 29579–29594, 2000.  
817

818 Peterson T. C., Folland C., Gruza G., Hogg W. Mokssit A., Plummer N. : Report on the  
819 activities of the working group on climate change detection and related rapporteurs 1998-  
820 2001. Geneva (Switzerland): WMO Rep. WCDMP 47, WMO-TD 1071, 2001.  
821

822 Philippon N., Mougou E. , Jarlan L. , and Frison P.-L.: Analysis of the linkages between  
823 rainfall and land surface conditions in the West African monsoon through CMAP, ERS-  
824 WSC, and NOAA-AVHR R data. *J. Geophys. Res.*, 110, D24115,  
825 doi:10.1029/2005JD006394, 2005.  
826

827 Reynolds, R. W. and Smith, T. M.: Improved global sea surface temperature analysis using  
828 optimum interpolation, *J. Climate*, 7, 929–948, 1994.  
829

830 Simmons A. S., Uppala D. D. and Kobayashi S.: ERA-interim: new ECMWF reanalysis  
831 products from 1989 onwards, *ECMWF Newsl.*, 110, 29–35, 2007.

832 Solmon F., Giorgi F., and Lioussé C.: Aerosol modeling for regional climate studies:  
833 application to anthropogenic particles and evaluation over a European/African domain, *Tellus*  
834 *B*, 58, 51–72, 2006.  
835



836 Sundqvist H. E., Berge E., and Kristjansson J. E.: The effects of domain choice on summer  
837 precipitation simulation and sensitivity in a regional climate model, *J. Climate*, 11, 2698–  
838 2712, 1999.

839

840 Sylla MB, Giorgi F, Stordal F.: Large-scale origins of rainfall and temperature bias in high  
841 resolution simulations over Southern Africa. *Climate Res.* 52: 193–211, DOI:  
842 10.3354/cr01044, 2012.

843

844 Tadross MA, Gutowski WJ Jr, Hewitson BC, Jack C, New M.: MM5 simulations of  
845 interannual change and the diurnal cycle of southern African regional climate. *Theor. Appl.*  
846 *Climatol.* 86(1–4):63–80, 2006.

847

848 Thanh N.-D., Fredolin T. T., Jerasorn S., Faye C., Long T.-T., Thanh N.-X., Tan P.-V., Liew  
849 J., Gemma N., Patama S., Dodo G. and Edwin A.: Performance evaluation of RegCM4 in  
850 simulating extreme rainfall and temperature indices over the CORDEX-Southeast Asia  
851 region. *Int. J. Climatol.* 37: 1634–1647. Published online 28 June 2016 in Wiley Online  
852 Library (wileyonlinelibrary.com) DOI: 10.1002/joc.4803, 2017.

853

854 Uppala S., Dee D., Kobayashi S., Berrisford P. and Simmons A.: Towards a climate data  
855 assimilation system: status update of ERA-interim, *ECMWF Newsl.*, 15, 12–18, 2008.

856

857 Wang, G., Yu, M., Pal, J. S., Mei, R., Bonan, G. B., Levis, S., and Thornton, P. E.: On the  
858 development of a coupled regional climate vegetation model RCM-CLM-CN-DV and its  
859 validation its tropical Africa, *Clim. Dynam.*, 46, 515–539, 2016.

860

861 You Q., Kang S., Aguilar E., Pepin N., Flügel W.-A., Yan Y. , Xu Y., Zhang Y. , and Huang  
862 J. : Changes in daily climate extremes in China and their connection to the large scale  
863 atmospheric circulation during 1961–2003, *Clim. Dyn.*, 36(11-12), 2399–2417,  
864 doi:10.1007/s00382-009-0735-0, 2010.

865

866 Zakey A. S., Solmon F., and Giorgi F.: Implementation and testing of a desert dust module in  
867 a regional climate model, *Atmos. Chem. Phys.*, 6, 4687–4704, [https://doi.org/10.5194/acp-6-](https://doi.org/10.5194/acp-6-4687-2006)  
868 4687-2006, 2006.

869  
870 Zeng X., Zhao M. and Dickinson R .E.: Intercomparison of bulk aerodynamic algorithms for  
871 the computation of sea surface fluxes using TOGA COARE and TAO DATA, *J. Climate*, 11,  
872 2628-2644, 1998.

873  
874 Zhang J, Wang W.C., and Wu L.: Land–atmosphere coupling and diurnal temperature range  
875 over the contiguous United States. *Geophys Res Lett* 36:L06706.  
876 doi:10.1029/2009GL037505, 2009.

877  
878 Zhang J. Y., Wu L. Y. and Dong W. : Land-atmosphere coupling and summer climate  
879 variability over East Asia, *J. Geophys. Res.*, 116,D05117, doi 10.1029/2010JD014714, 2011.

880  
881  
882  
883  
884  
885  
886  
887  
888  
889  
890  
891  
892  
893  
894  
895  
896  
897

898 **TABLES AND FIGURES.**

899

Extreme indices		Definition	Units
Extreme Rainfall Indices			
1	R1mm	Number of wet days (daily precipitation $\geq 1$ mm)	day
2	SDII	The amount of precipitation mean on wet days (daily precipitation $\geq 1$ mm)	mm.day <sup>-1</sup>
3	CDD	Maximum number of consecutive dry days (daily precipitation $< 1$ mm.day <sup>-1</sup> )	day
4	CWD	Maximum number of consecutive wet days (daily precipitation $\geq 1$ mm.day <sup>-1</sup> )	day
5	RX1day	The maximum one-day precipitation accumulation	mm
6	R95pTOT	Precipitation percent due to very heavy precipitation days.	%
Extreme temperature indices			
7	TXn	Minimum value of daily maximum temperature	°C
8	TXx	Maximum value of daily maximum temperature	°C
9	TNn	Minimum value of daily minimum temperature	°C
10	TNx	Maximum value of daily minimum temperature	°C

900

901 **Table1:** The 10 extreme climate indices used in this study.

902

903

904

905

		Central Sahel		West Sahel		guinea		West Africa	
		MB	PCC	MB	PCC	MB	PCC	MB	PCC
R1mm	TRMM_2003	-6.76	0.98	-3.15	0.99	8.89	0.99	-1.12	0.98
	CTRL_2003	33.17	0.98	-5.25	0.96	53.16	0.96	22.18	0.96
	TRMM_2004	-7.51	0.98	-3.42	0.99	10.44	0.98	-1.34	0.98
	CTRL_2004	29.50	0.98	1.34	0.96	55.46	0.96	23.85	0.95
SDII	TRMM_2003	2.67	0.96	0.22	0.94	-5.24	0.95	1.20	0.86
	CTRL_2003	-7.52	0.97	-9.95	0.94	-13.62	0.77	-7.67	0.73
	TRMM_2004	2.07	0.96	0.45	0.96	-6.44	0.94	1.16	0.86
	CTRL_2004	-7.01	0.97	-9.37	0.94	-14.65	0.81	-7.59	0.77
CDD	TRMM_2003	1.21	0.95	0.89	0.93	-0.93	0.94	-2.29	0.92
	CTRL_2003	0.93	0.90	14.49	0.91	-7.84	0.66	2.63	0.85
	TRMM_2004	2	0.95	1.58	0.96	-3.17	0.92	-1.75	0.94
	CTRL_2004	4.75	0.91	17.51	0.95	-9.43	0.68	6.99	0.89
CWD	TRMM_2003	-0.48	0.92	0.80	0.94	2.47	0.92	0.37	0.90
	CTRL_2003	45.56	0.83	18.44	0.75	59.21	0.88	31.20	0.81
	TRMM_2004	-0.68	0.92	0.97	0.92	2.38	0.89	0.26	0.87
	CTRL_2004	36.78	0.79	20.48	0.78	60.51	0.82	29.74	0.79
RX1day	TRMM_2003	35.78	0.92	25.31	0.89	14.31	0.86	26.02	0.84
	CTRL_2003	-26.46	0.78	-38.07	0.91	-30.28	0.54	-20.08	0.50
	TRMM_2004	31.66	0.91	20.19	0.91	10	0.88	22.19	0.85
	CTRL_2004	-22.89	0.46	-36.67	0.88	-42.44	0.42	-20.23	0.40
R95pTOT	TRMM_2003	23.19	0.92	13.31	0.94	-0.23	0.96	16.54	0.91
	CTRL_2003	-27.67	0.67	-33.39	0.77	-43.22	0.65	-29.12	0.59
	TRMM_2004	23.26	0.91	12.32	0.94	-0.93	0.95	18.54	0.91
	CTRL_2004	-24.38	0.46	-31.75	0.80	-46.61	0.60	-27.45	0.55

907

908 **Table 2:** The pattern correlation coefficient (PCC) and the mean bias (MB) of R1mm (in  
909 day), SDII (in mm.day-1), CDD (in day), CWD (in day), RX1day (in mm) and R95pTOT (in  
910 %) indices for TRMM observation and their corresponding control experiments (initialized  
911 with initial soil moisture of ERA20C reanalysis) with respect to CHIRPS, calculated over  
912 Guinea coast, central Sahel, west Sahel and the entire West African domain for JJAS 2003  
913 and JJAS 2004.

914

		Central Sahel		West Sahel		guinea		West Africa	
		MB	PCC	MB	PCC	MB	PCC	MB	PCC
TXx	TRMM_2003	-2.17	0.99	-3.05	0.99	-4	0.99	-2.77	0.99
	CTRL_2003	2.10	0.99	3.02	0.99	-1.34	0.99	0.32	0.99
	TRMM_2004	-2.44	0.99	-3.86	0.99	-3.84	0.99	-2.94	0.99
	CTRL_2004	1.14	0.99	2.02	0.99	-1.41	0.99	-0.16	0.99
TXn	TRMM_2003	0.31	0.99	-1.48	0.99	-0.70	0.99	0.50	0.99
	CTRL_2003	5.12	0.99	6.56	0.99	3.76	0.99	5.65	0.99
	TRMM_2004	-0.76	0.99	-1.73	0.99	-1.38	0.99	-0.32	0.99
	CTRL_2004	3.43	0.99	5.44	0.99	2.75	0.99	4.14	0.99
TNn	TRMM_2003	3.08	0.99	3.43	0.99	1.28	0.99	3.15	0.99
	CTRL_2003	2.37	0.99	3.30	0.99	1.53	0.99	1.45	0.99
	TRMM_2004	3.28	0.99	2.98	0.99	1.20	0.99	3.11	0.99
	CTRL_2004	2.09	0.99	2.55	0.99	1.28	0.99	0.71	0.99
TNx	TRMM_2003	-0.69	0.99	-1.79	0.99	-3.11	0.99	-1.62	0.99
	CTRL_2003	-1.91	0.99	-2.86	0.99	-3.35	0.99	-3.85	0.99
	TRMM_2004	-0.82	0.99	-1.43	0.99	-3.14	0.99	-1.71	0.99
	CTRL_2004	-1.90	0.99	-2.54	0.99	-3.32	0.99	-3.99	0.99

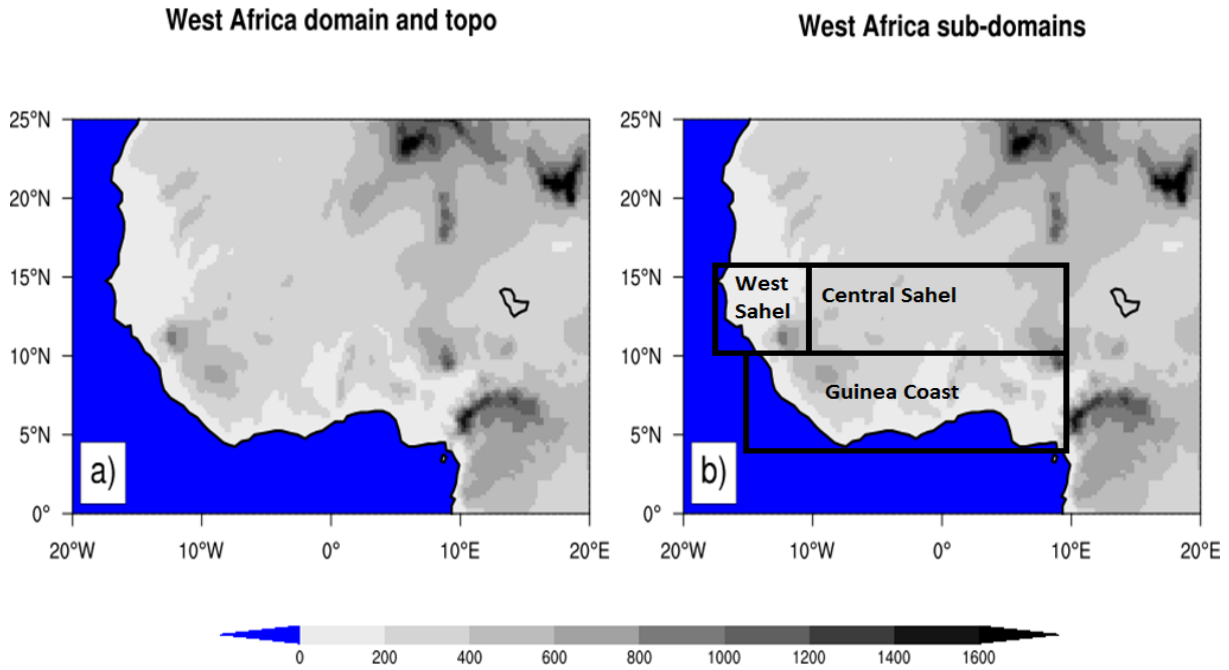
916

917 **Table 3:** The pattern correlation coefficient (PCC) and the mean bias (MB in°C) of TXx,  
918 TXn, TNn and TNx indices from the EIN reanalysis and their corresponding control  
919 experiments (initialized with initial soil moisture of ERA20C reanalysis) with respect to GTS,  
920 calculated for Guinea coast, central Sahel, west Sahel and the entire West African domain for  
921 JJAS 2003 and JJAS 2004.

922

923

924



925

926

927 **Figure 1:** Topography of the West African domain. The analysis of the model result has an  
928 emphasis on the whole West African domain and the three subregions Guinea coast, central  
929 Sahel and west Sahel, which are marked with black boxes.

930

931

932

933

934

935

936

937

938

939

940

941

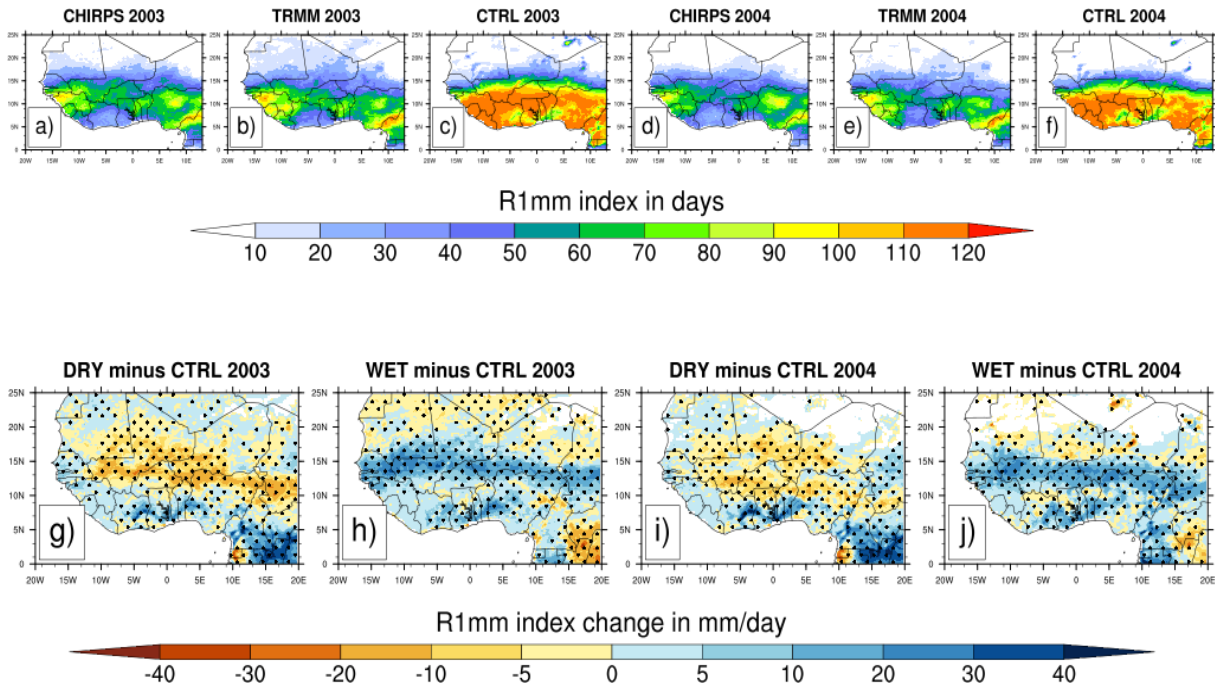
942

943

944

945

946



947

948

949 **Figure2:** Observed 4-month averaged (JJAS) mean values of the number of the wet days  
950 (R1mm index in days) from CHIRPS (a and d) and TRMM(b and e) observations for JJAS  
951 2003 and JJAS 2004 and their corresponding simulated control (CTRL) experiments (c and f)  
952 initialized with initial soil moisture of the reanalysis of ERA20C (first panel) and changes in  
953 R1mm index in days (second panel) for JJAS 2003 and JJAS 2004, from dry (g and i) and wet  
954 (h and j) experiments with respect to the corresponding control experiments. Areas with  
955 values passing the 10% significance test are dotted.

956

957

958

959

960

961

962

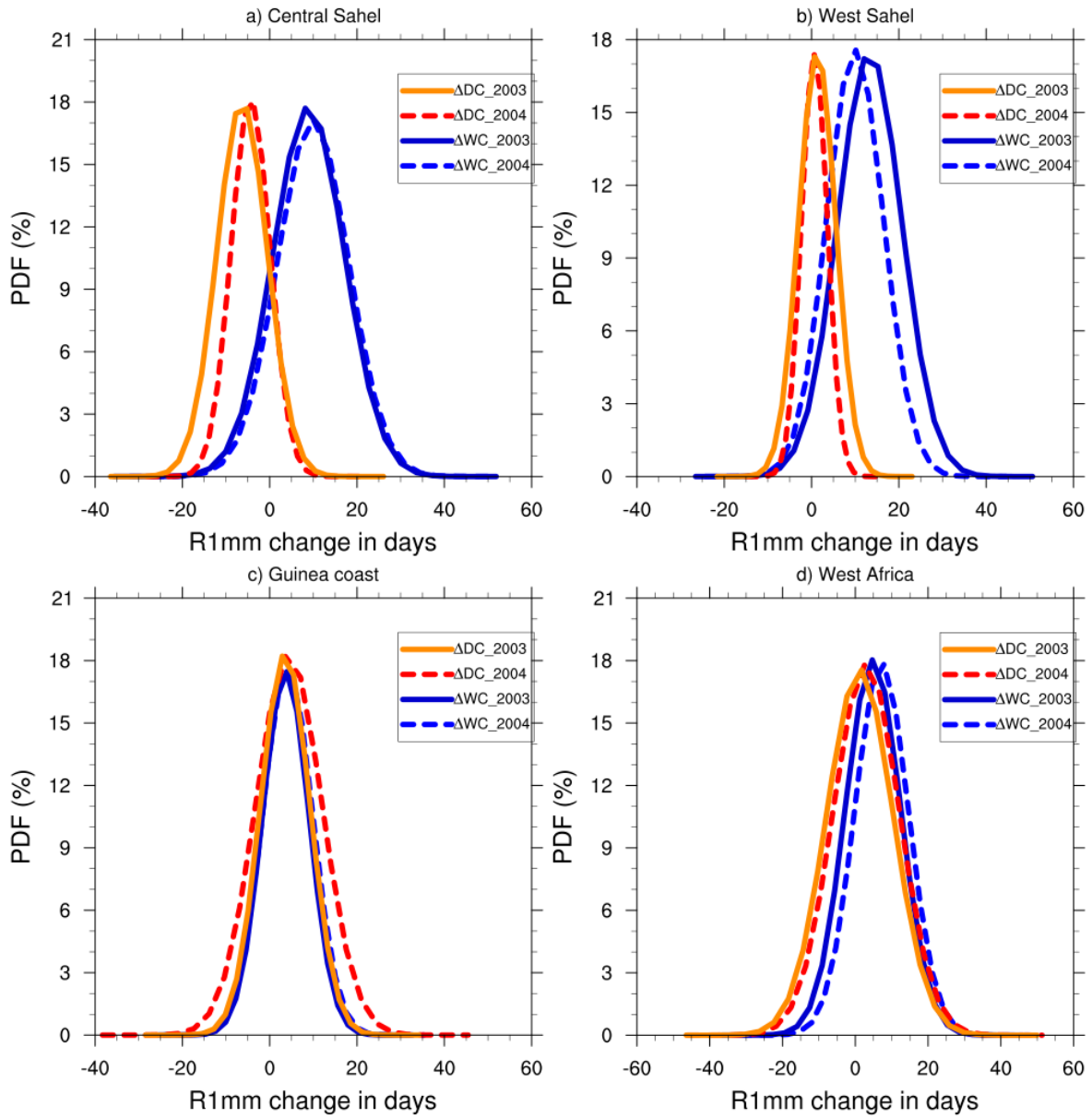
963

964

965

966





968

969

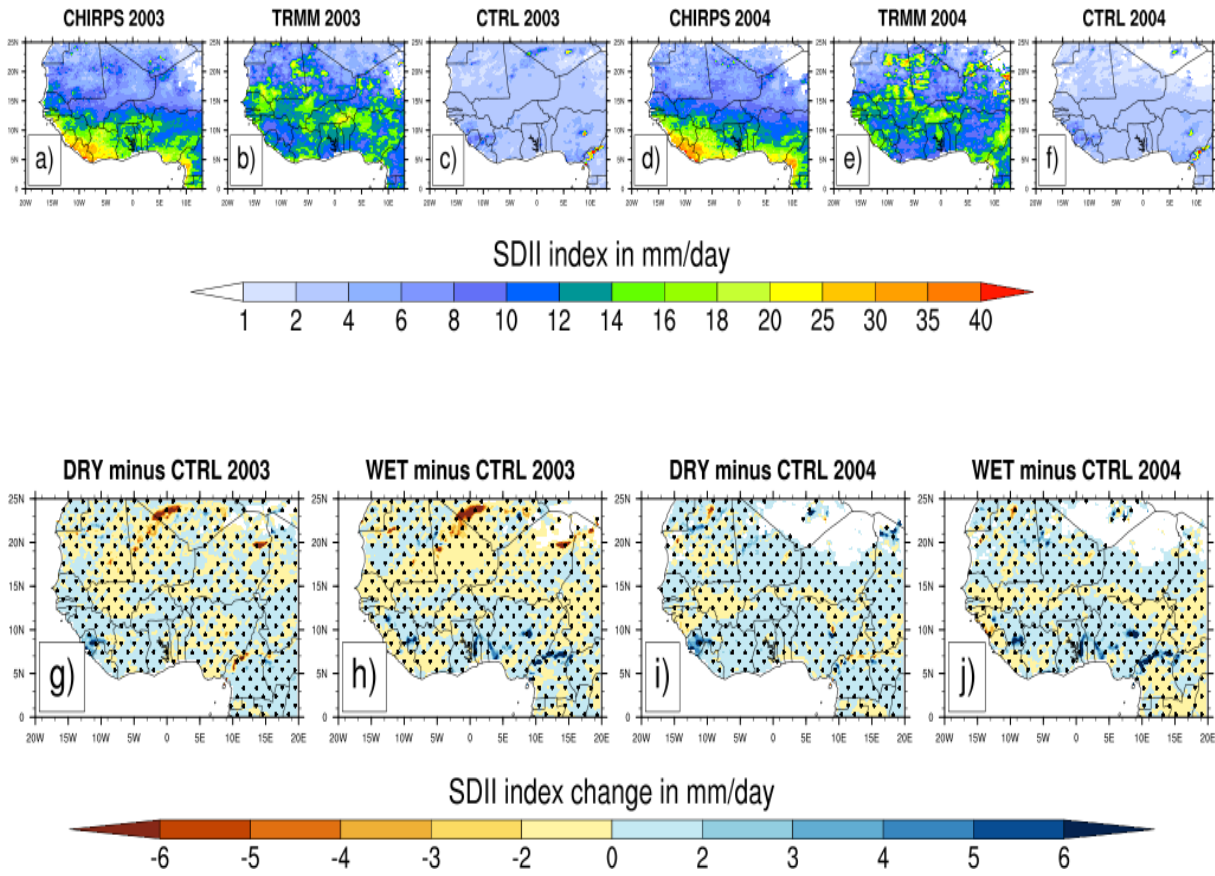
970 **Figure3:** PDF distributions (%) of mean values of the number of the wet days change in JJAS  
 971 2003 and JJAS 2004, over (a) central Sahel , (b) West Sahel, (c) Guinea and (d) West Africa  
 972 derived from dry ( $\Delta DC$ ) and wet ( $\Delta WC$ ) experiments with respect to their corresponding  
 973 control experiment.

974

975

976

977



979

980

981 **Figure4:** Same as Fig. 2 but for the SDII index (in mm.day<sup>-1</sup>).

982

983

984

985

986

987

988

989

990

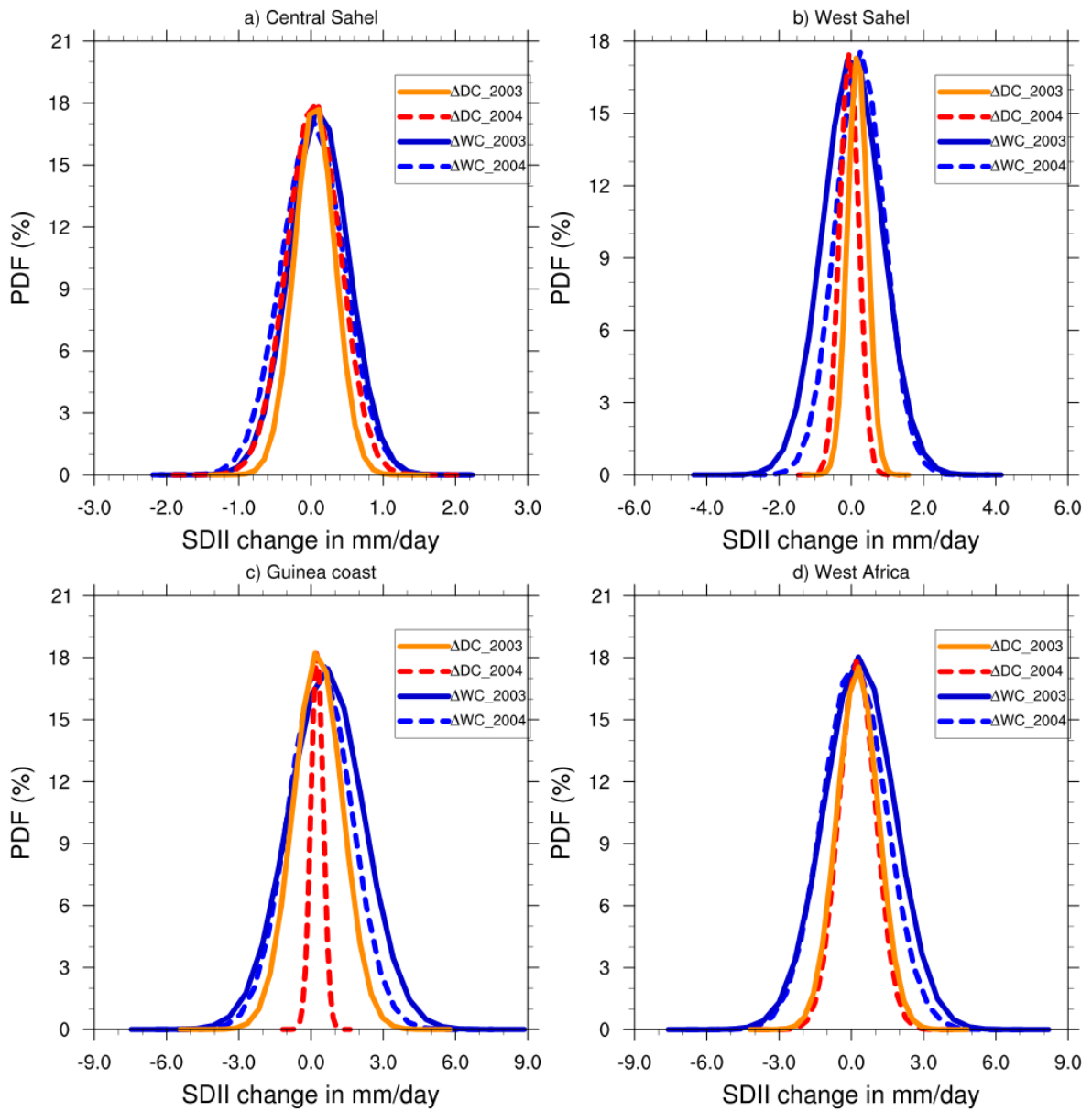
991

992

993

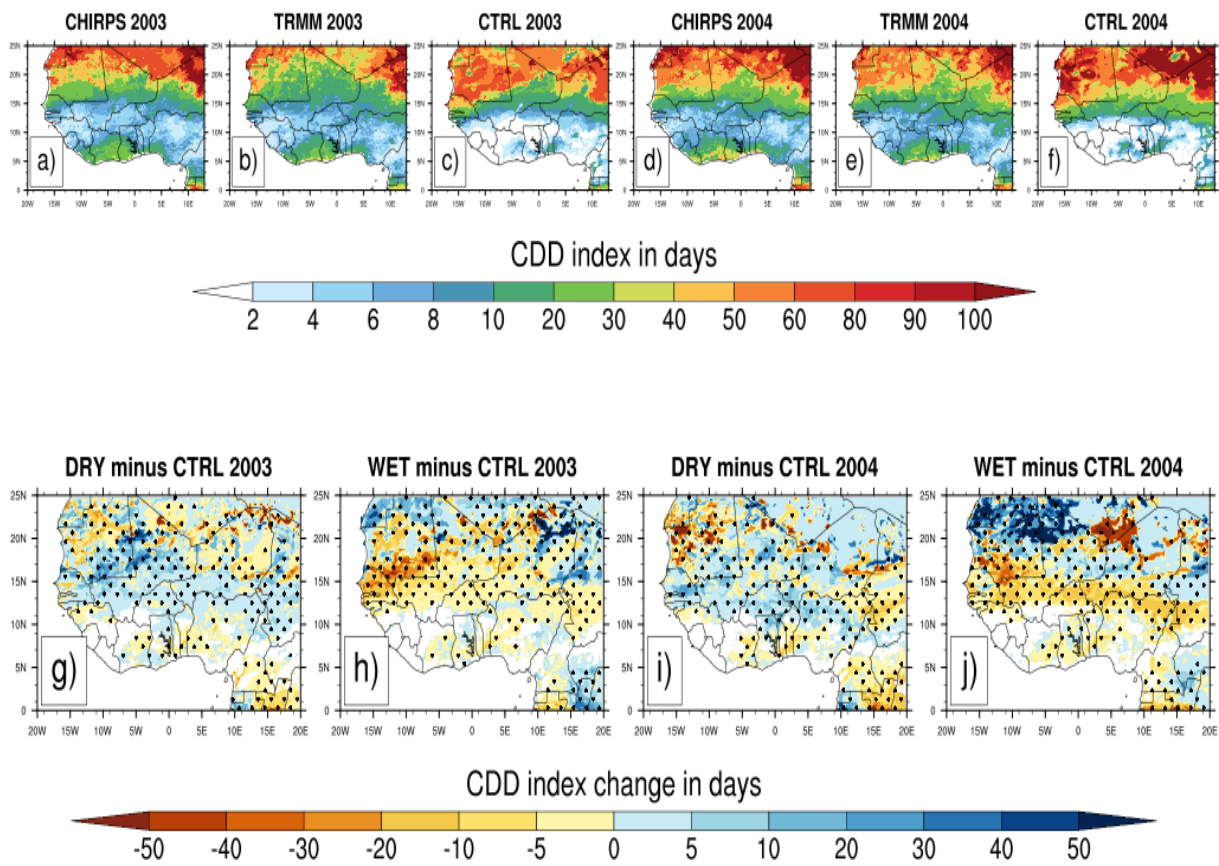
994

995



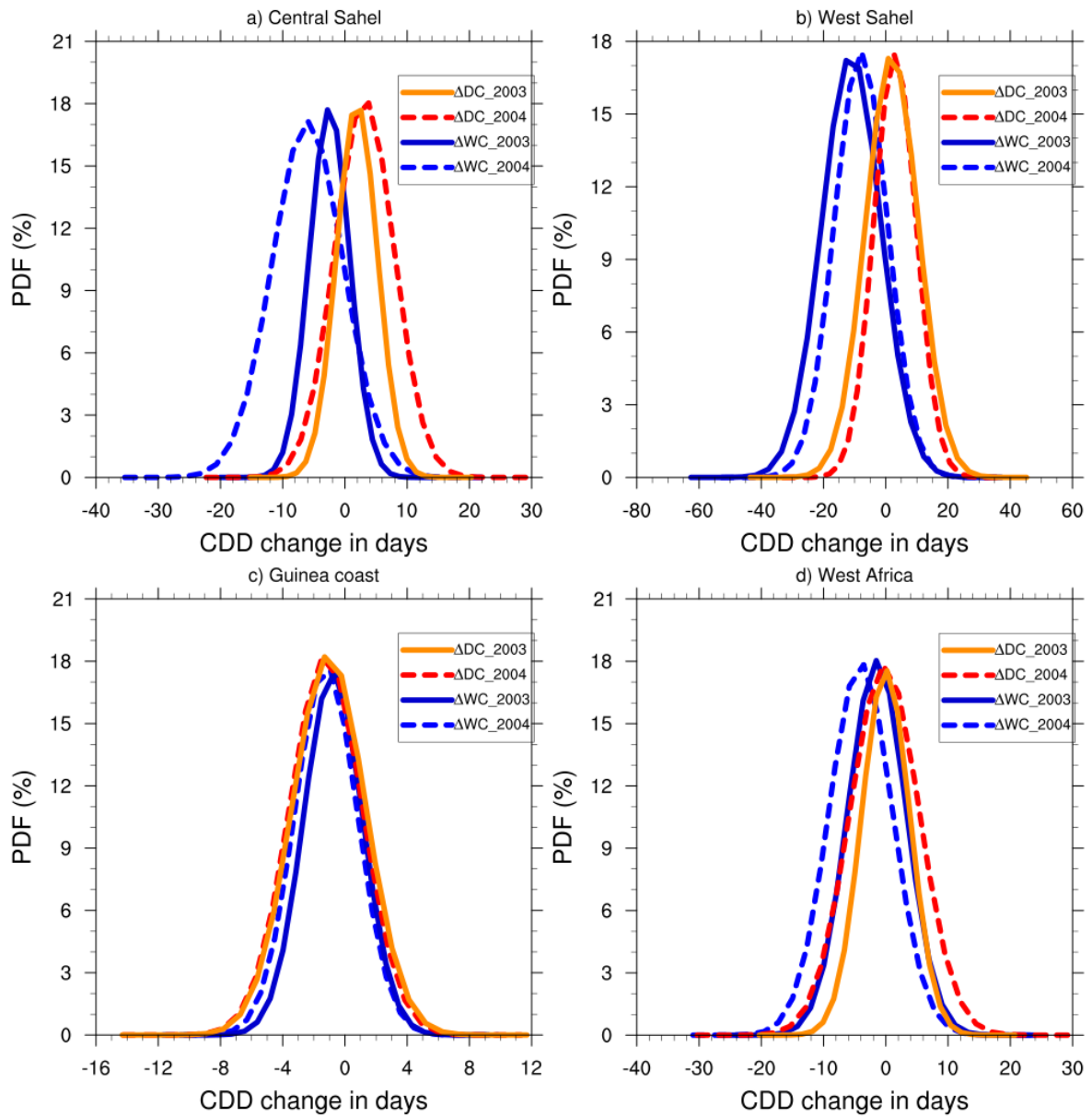
996  
 997  
 998  
 999  
 1000  
 1001  
 1002  
 1003  
 1004  
 1005  
 1006  
 1007

**Figure 5:** Same as Fig. 3 but for the SDII index (in mm.day<sup>-1</sup>).



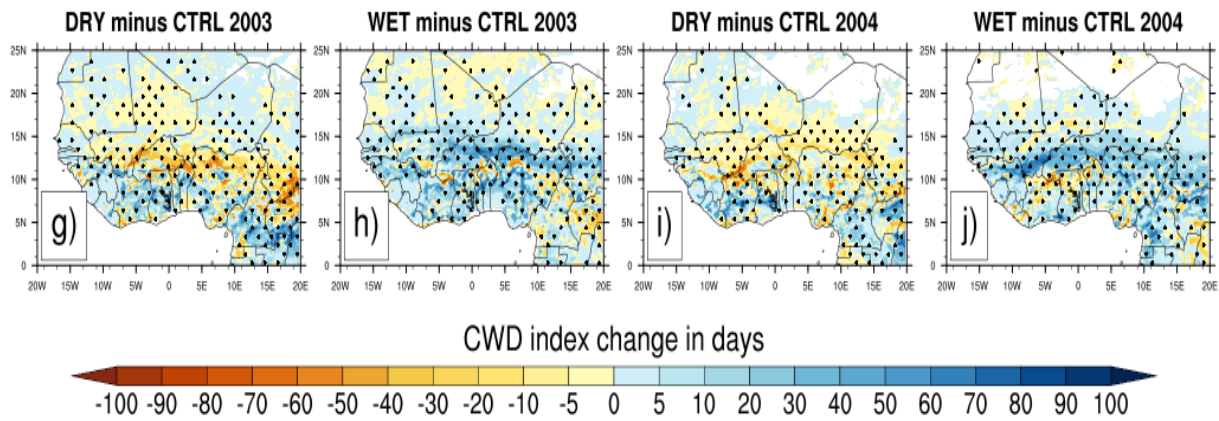
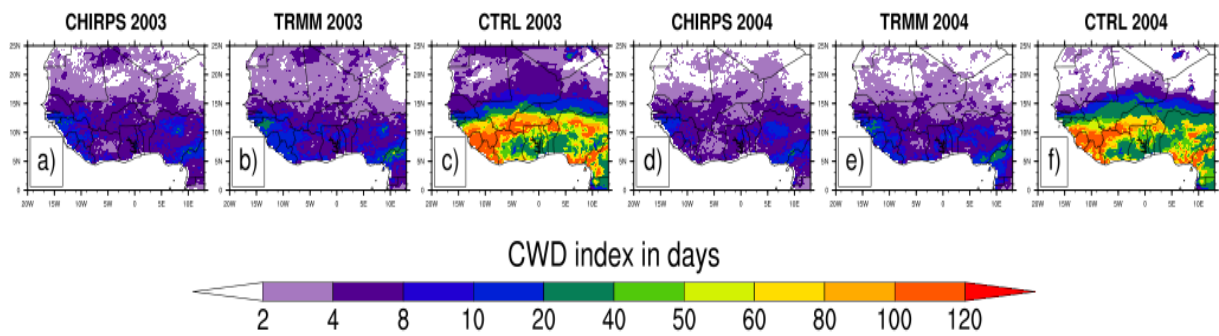
1008  
 1009  
 1010  
 1011  
 1012  
 1013  
 1014  
 1015  
 1016  
 1017  
 1018  
 1019  
 1020  
 1021  
 1022  
 1023  
 1024

**Figure 6:** Same as Fig. 2 but for the CDD index (in day).



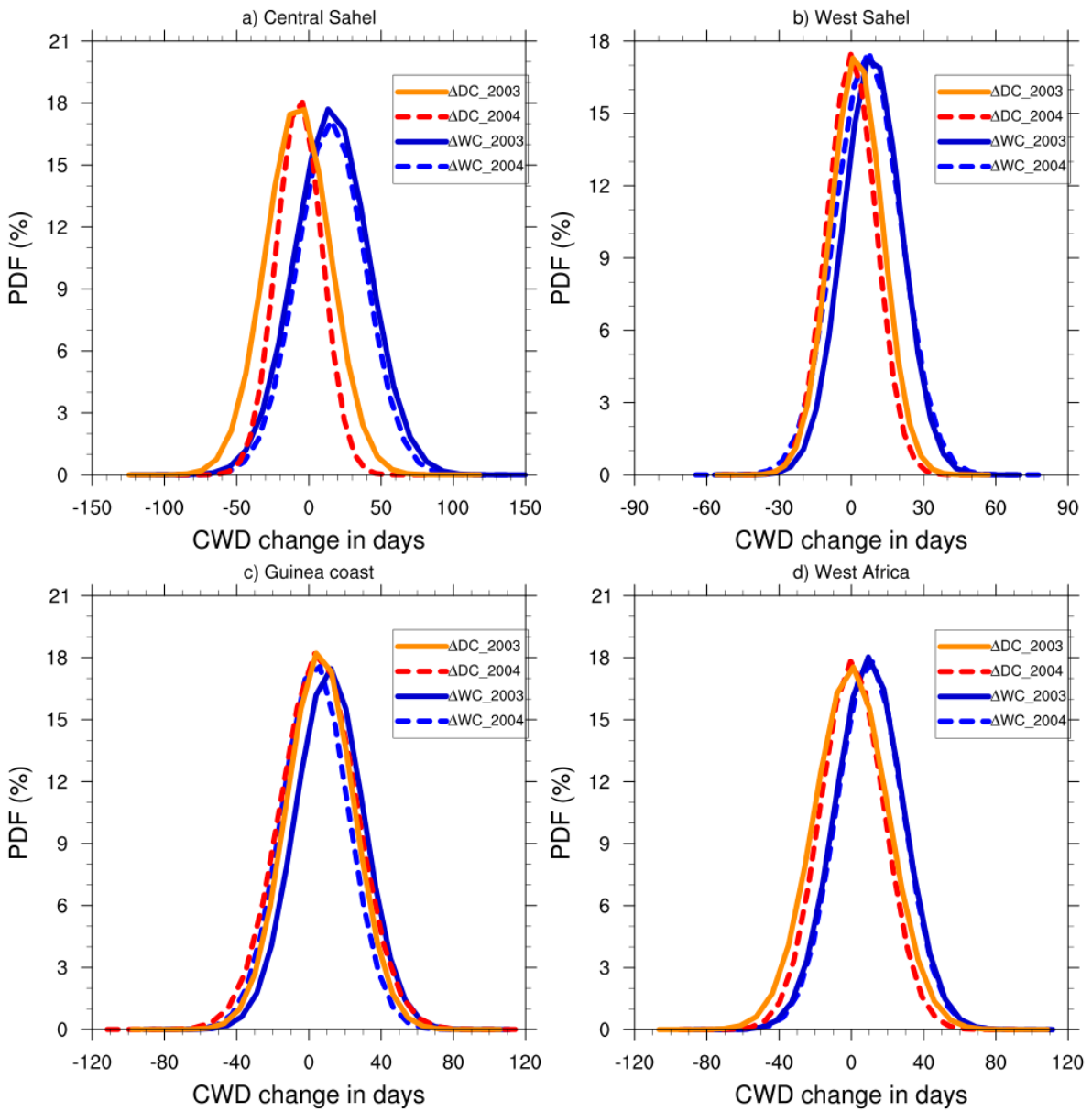
1025  
 1026  
 1027  
 1028  
 1029  
 1030  
 1031  
 1032  
 1033  
 1034  
 1035

**Figure 7:** Same as Fig. 3 but for the CDD index (in day).



1036  
 1037  
 1038  
 1039  
 1040  
 1041  
 1042  
 1043  
 1044  
 1045  
 1046  
 1047  
 1048  
 1049  
 1050  
 1051  
 1052  
 1053  
 1054

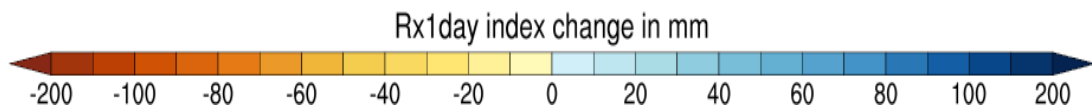
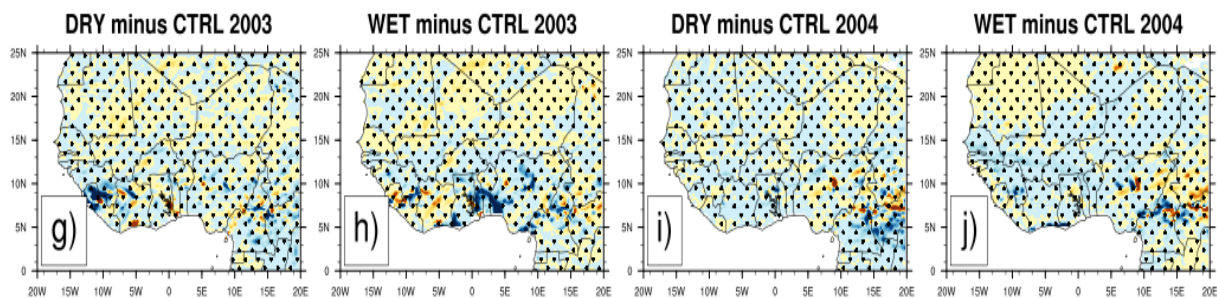
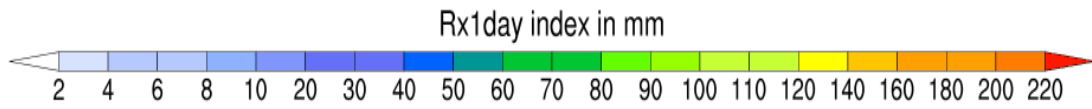
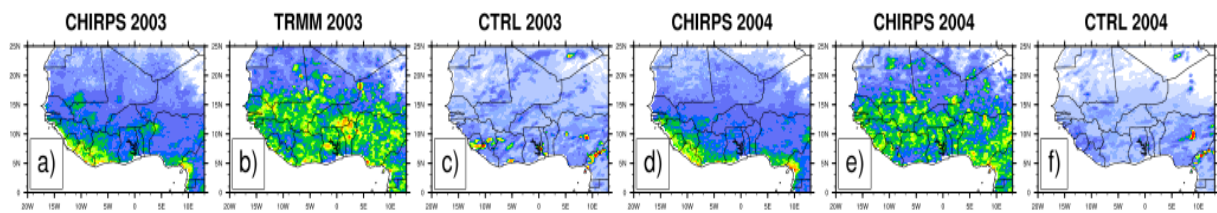
**Figure 8:** Same as Fig. 2 but for the CWD index (in day).



1055  
 1056  
 1057  
 1058  
 1059  
 1060  
 1061  
 1062  
 1063  
 1064  
 1065  
 1066

**Figure 9:** Same as Fig. 3 but for the CWD index (in day).





1067

1068

1069 **Figure 10:** Same as Fig. 2 but for the RX1day index (in mm).

1070

1071

1072

1073

1074

1075

1076

1077

1078

1079

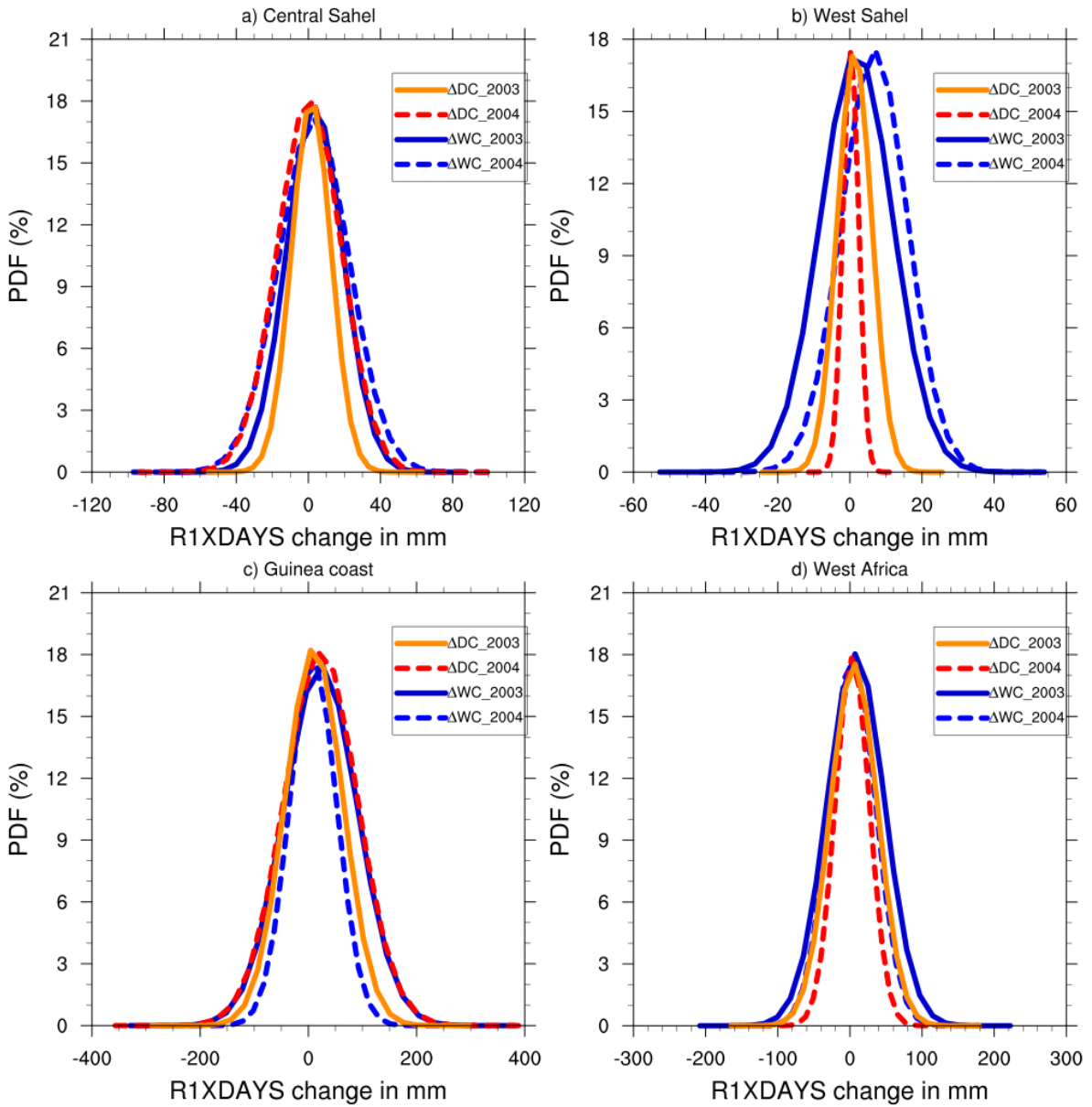
1080

1081

1082

1083

1084



1085

1086

1087

1088 **Figure 11:** Same as Fig. 3 but for the RX1DAY index (in mm).

1089

1090

1091

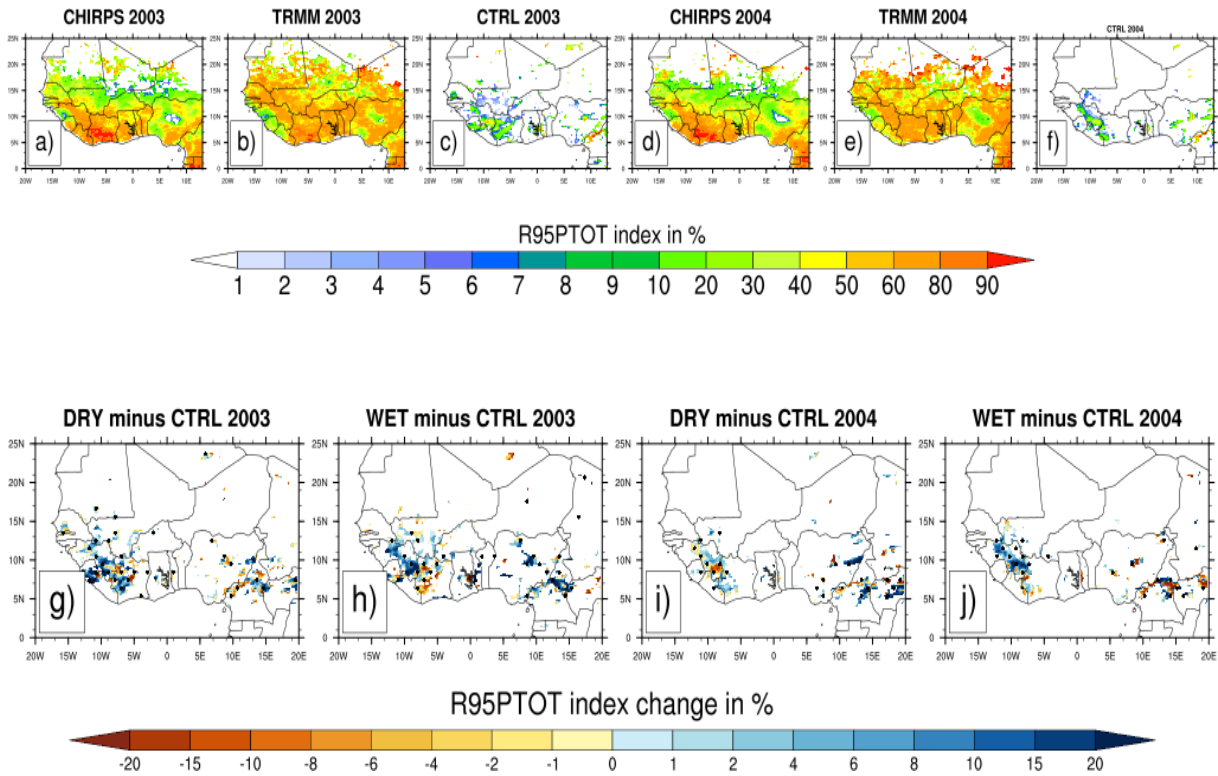
1092

1093

1094

1095

1096



1097

1098

1099 **Figure 12:** Same as Fig. 2 but for the R95pTOT index (in %).

1100

1101

1102

1103

1104

1105

1106

1107

1108

1109

1110

1111

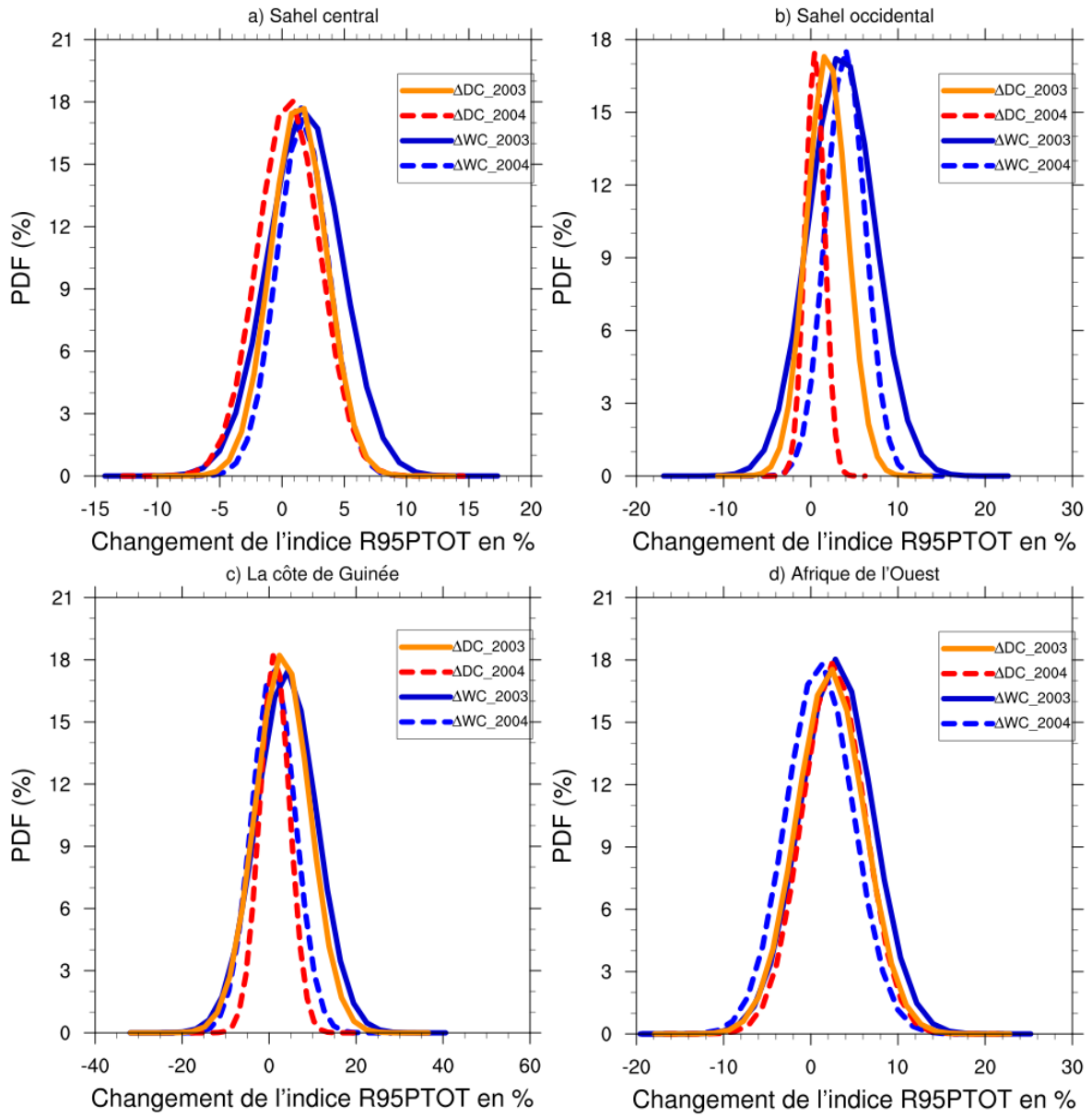
1112

1113

1114

1115

1116



1117

1118 **Figure 13:** Same as Fig. 3 but for the R95pTOT index (in %).

1119

1120

1121

1122

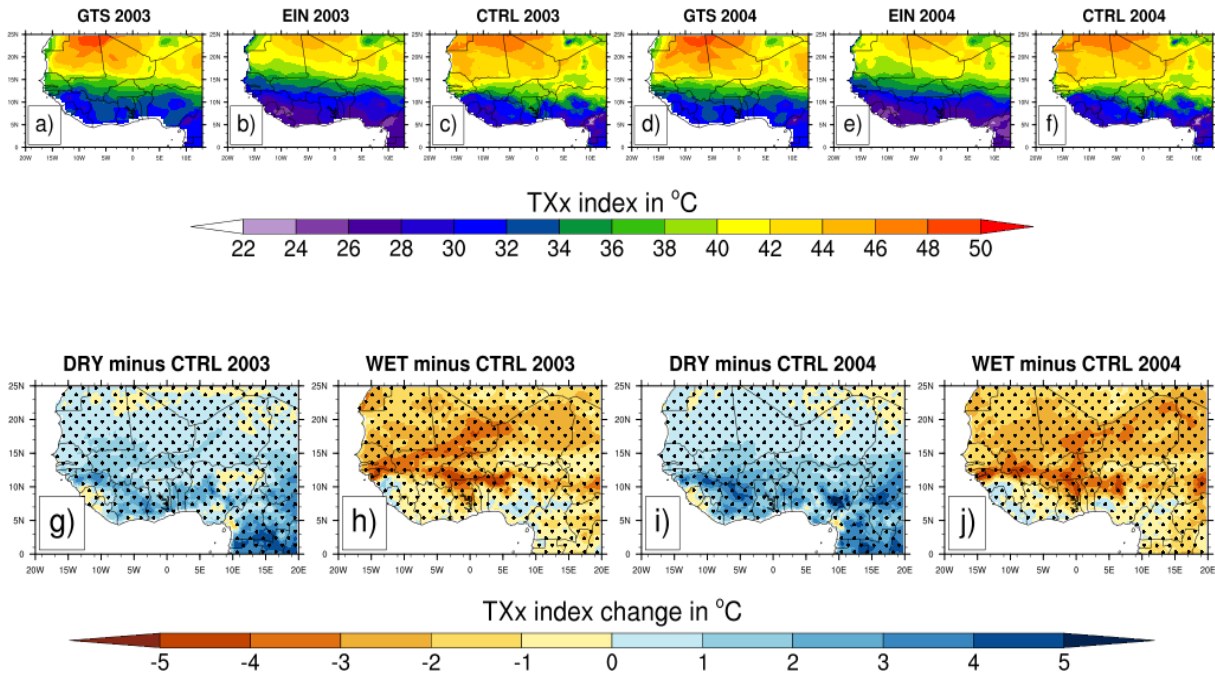
1123

1124

1125

1126

1127



1128

1129 **Figure 14:** Observed 4-month averaged (JJAS) maximum value of daily maximum

1130 temperature (TXx index in°C) from GTS observation (a and d) and The EIN reanalysis (b

1131 and e) for JJAS 2003 and JJAS 2004 and their corresponding simulated control (CTRL)

1132 experiments (c and f) initialized with the initial soil moisture of the ERA20C reanalysis (first

1133 panel) and changes in TXx index in°C (second panel) for JJAS 2003 and JJAS 2004, from dry

1134 (g and i) and wet (h and j) experiments with respect to the corresponding control experiments.

1135 Areas with values passing the 10% significance test are dotted.

1136

1137

1138

1139

1140

1141

1142

1143

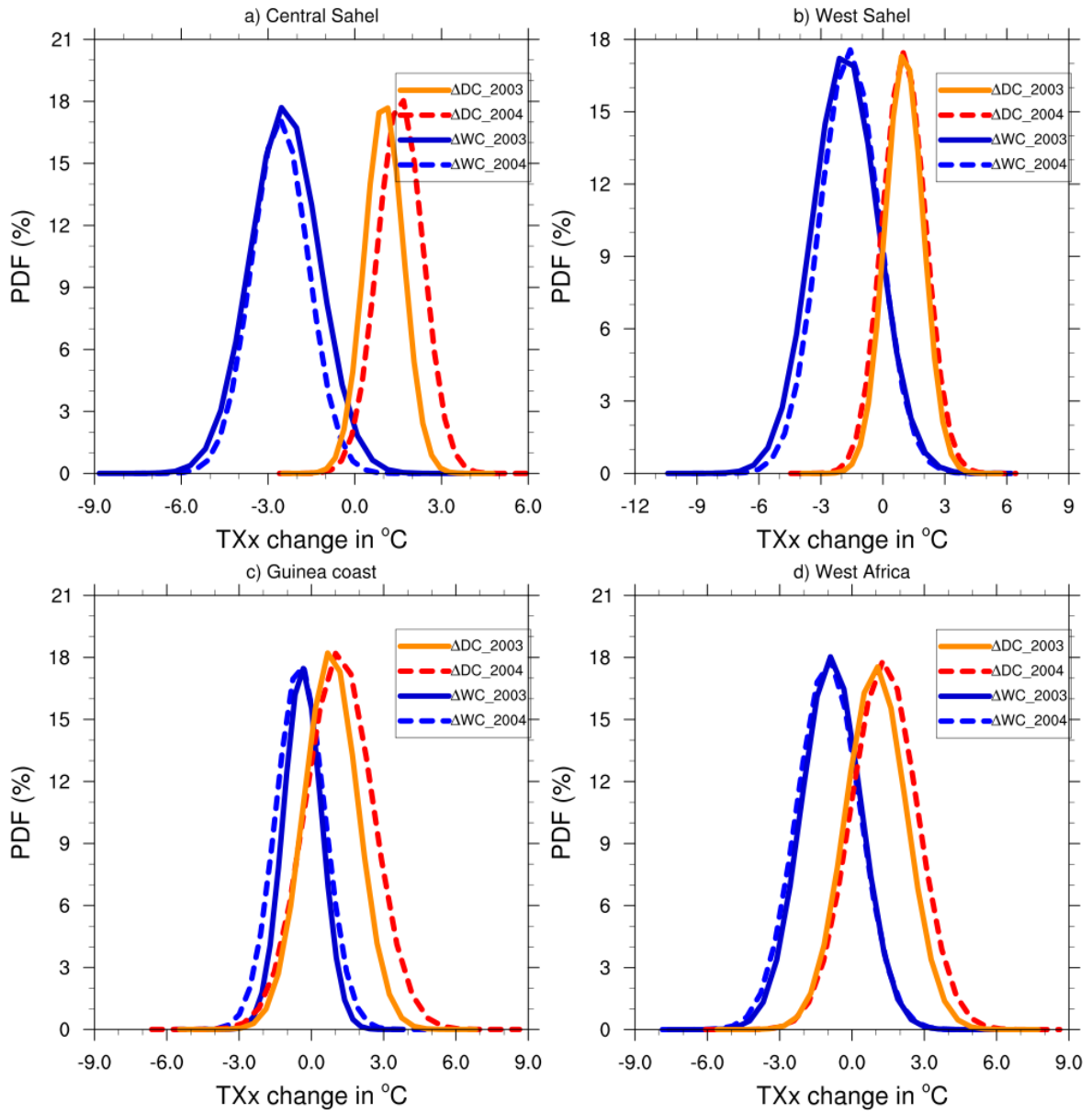
1144

1145

1146

1147

1148



1150

1151

1152 **Figure 15:** PDF distributions (%) of change in maximum value of daily maximum

1153 temperature (TXx index, in °C) for JJAS 2003 and JJAS 2004, over (a) central Sahel , (b)

1154 West Sahel, (c) Guinea and (d) West Africa derived from dry ( $\Delta DC$ ) and wet ( $\Delta WC$ )

1155 experiments compared to their corresponding control experiment.

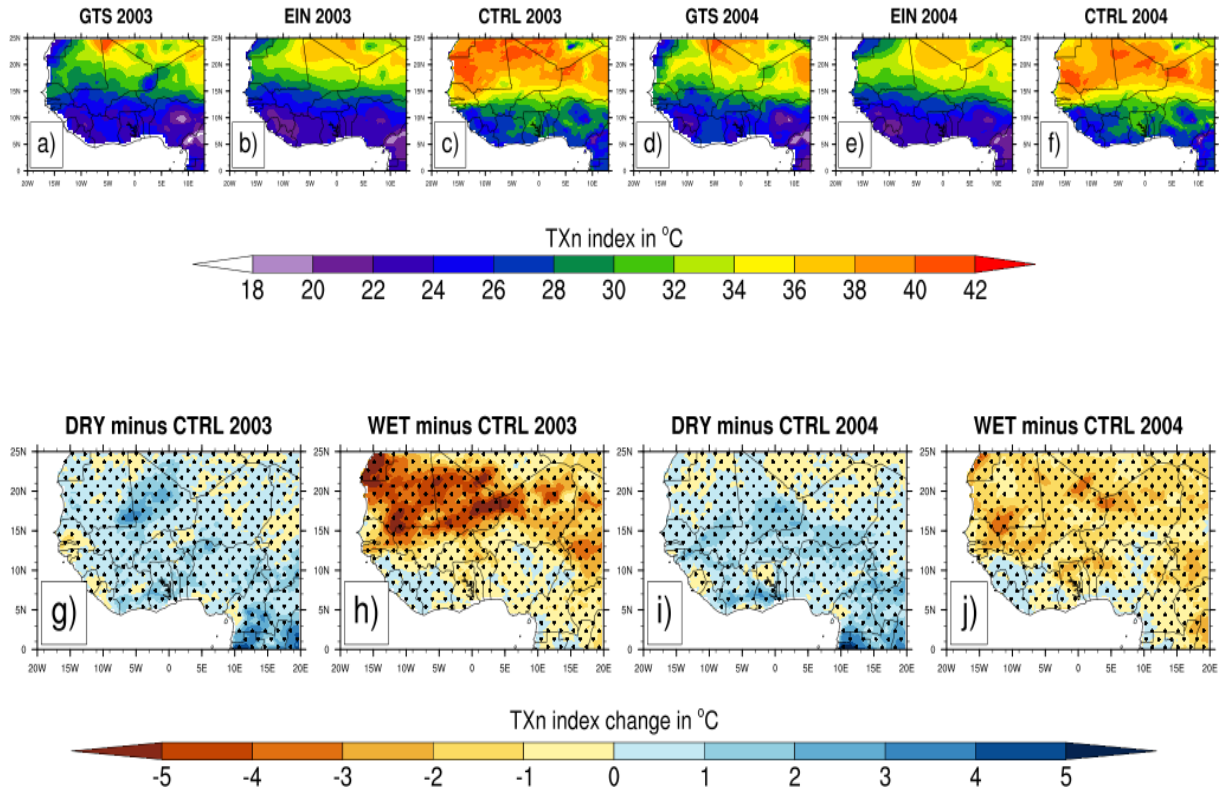
1156

1157

1158

1159

1160



1161

1162

1163

1164 **Figure 16:** Same as Fig. 14 but for the TXn index

1165

1166

1167

1168

1169

1170

1171

1172

1173

1174

1175

1176

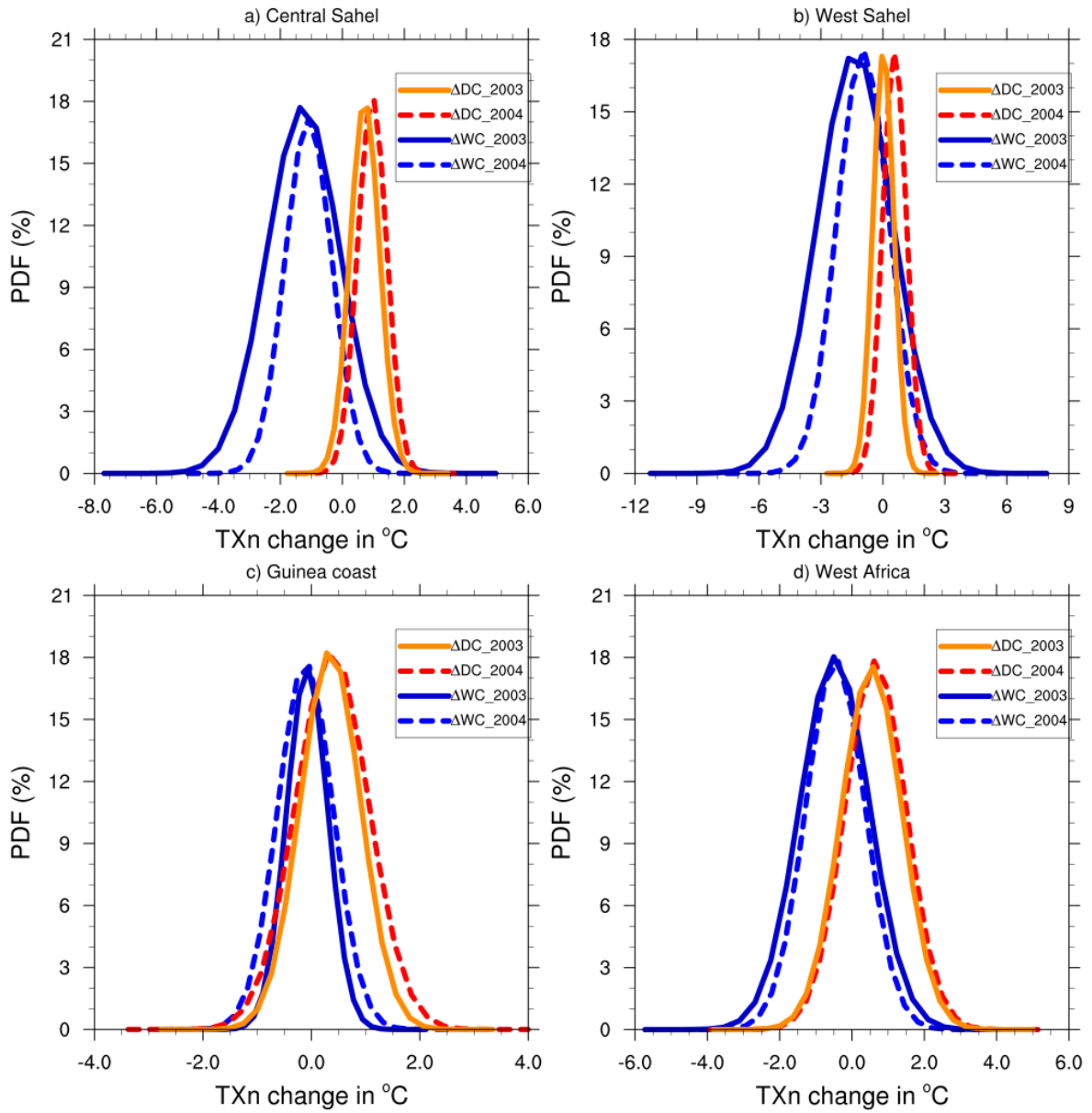
1177

1178

1179



1180



1181

1182

1183

1184

1185 **Figure 17:** Same as Fig. 15 but for the TXn index.

1186

1187

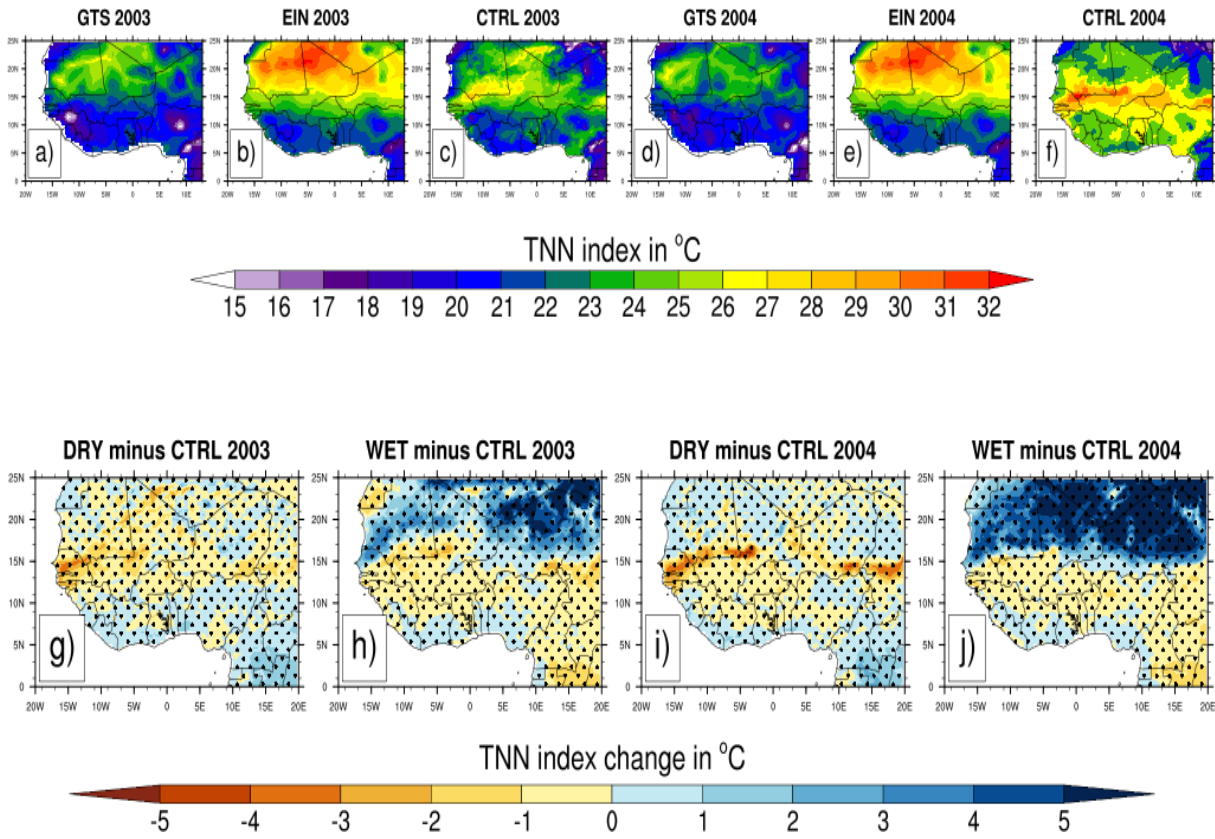
1188

1189

1190

1191

1192



1193

1194

1195

1196 **Figure 18:** Same as Fig. 14 but for the TNN index.

1197

1198

1199

1200

1201

1202

1203

1204

1205

1206

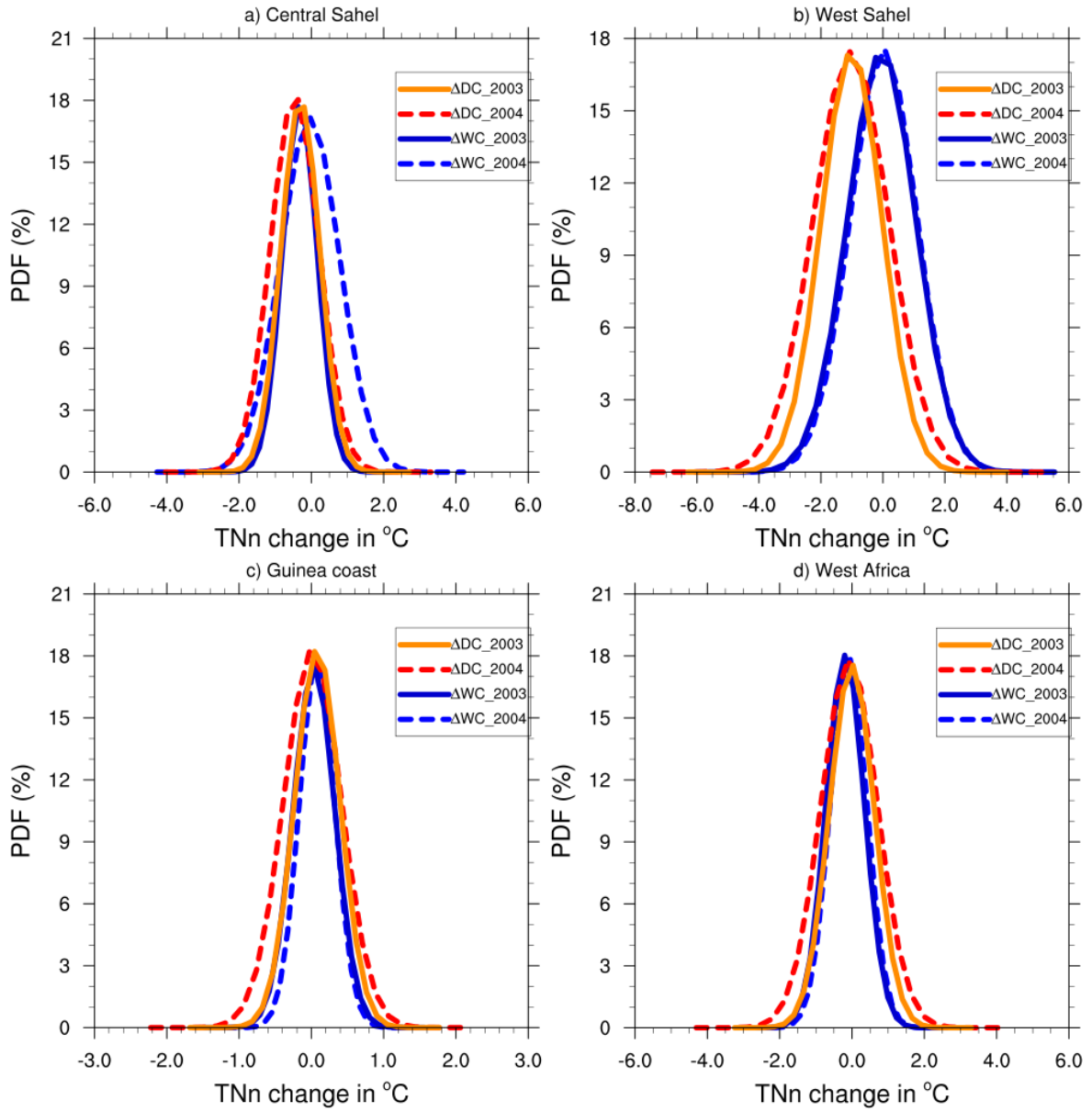
1207

1208

1209

1210

1211



1212

1213

1214

1215

1216 **Figure 19:** Same as Fig. 14 but for the TNn index.

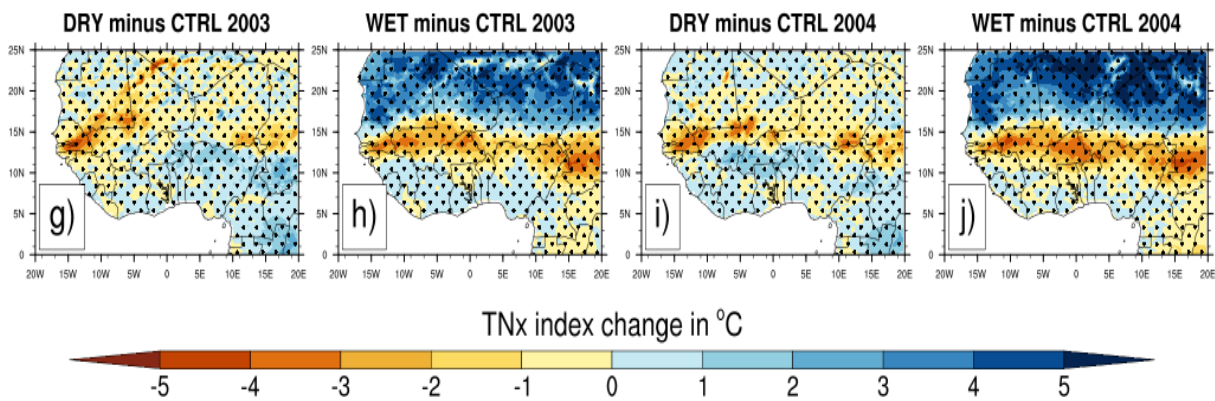
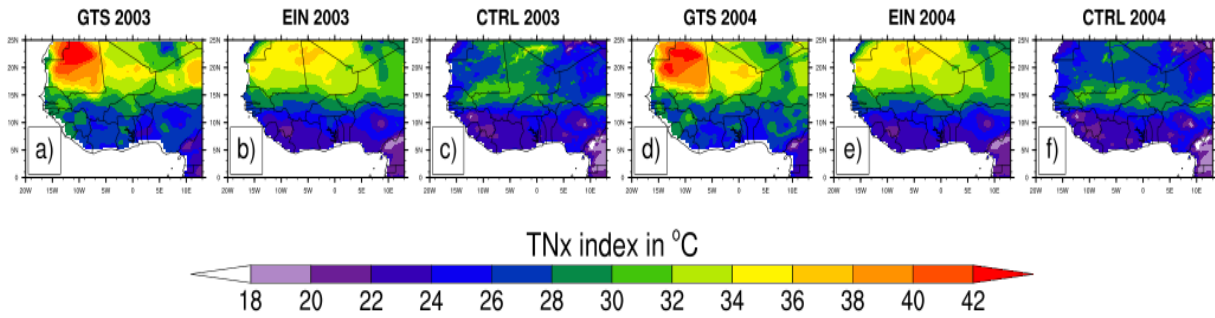
1217

1218

1219

1220

1221



1222

1223

1224 **Figure 20:** Same as Fig. 14 but for the TNx index

1225

1226

1227

1228

1229

1230

1231

1232

1233

1234

1235

1236

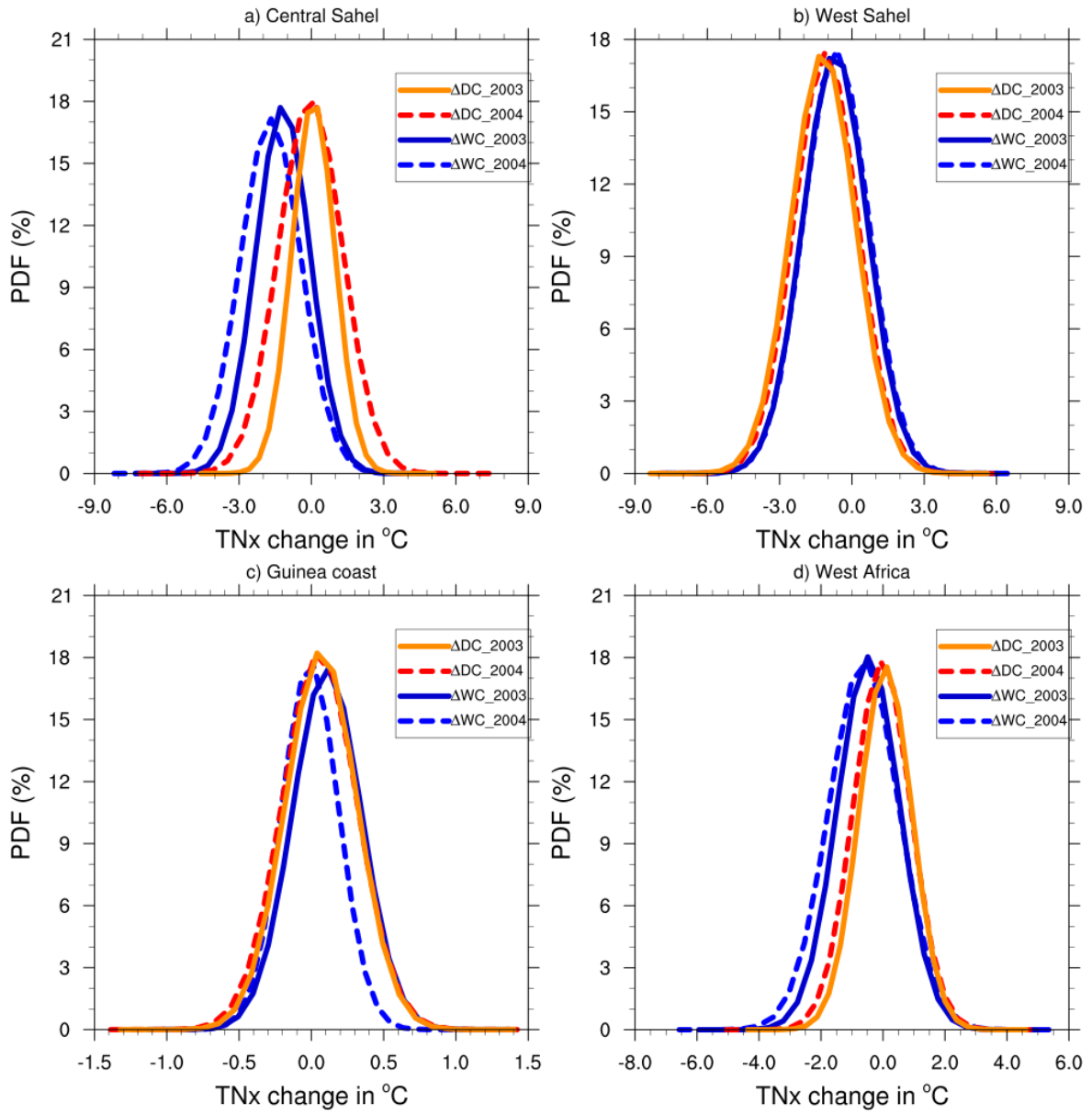
1237

1238

1239

1240

1241



1242

1243

1244 **Figure 21:** Same as Fig. 15 but for the TNx index.

1245

1246

1247